Inorganic Chemistry

Article

pubs.acs.org/IC

Functionalized Bis-Cyclometalated Alkynylgold(III) Complexes: Synthesis, Characterization, Electrochemistry, Photophysics, Photochemistry, and Electroluminescence Studies

Vonika Ka-Man Au, Daniel Ping-Kuen Tsang, Keith Man-Chung Wong, Mei-Yee Chan,* Nianyong Zhu, and Vivian Wing-Wah Yam*

Institute of Molecular Functional Materials [Areas of Excellence Scheme, University Grants Committee (Hong Kong)] and Department of Chemistry, The University of Hong Kong, Pokfulam Road, Hong Kong, P. R. China

Supporting Information

ABSTRACT: A series of luminescent alkynylgold(III) complexes containing various tridentate bis-cyclometalating ligands derived from 2,6-diphenylpyridine (R-C^N^C), [Au(R-C^N^C)(C≡C—C_6H_4—R′)] has been successfully synthesized and characterized. Complexes **1** and **6** have been determined by X-ray crystallography. Electrochemical studies show a ligand-centered reduction that originated from the tridentate R-C^N^C pincer ligands and an alkynyl-centered oxidation. The photophysical properties of the complexes have been studied in detail by electronic absorption and emission studies. Tunable photoluminescence behaviors have been observed, with the emission maxima spanning through the visible region from 476 to 669 nm in dichloromethane at room temperature, and the complexes were also found to be emissive in various media at both room and low temperatures. Transient absorption studies have been conducted to investigate the excited state properties of the complexes. Furthermore, selected complexes have been incorporated into the emissive layer (EML) of organic light-emitting devices (OLEDs) and have demonstrated interesting electroluminescence.

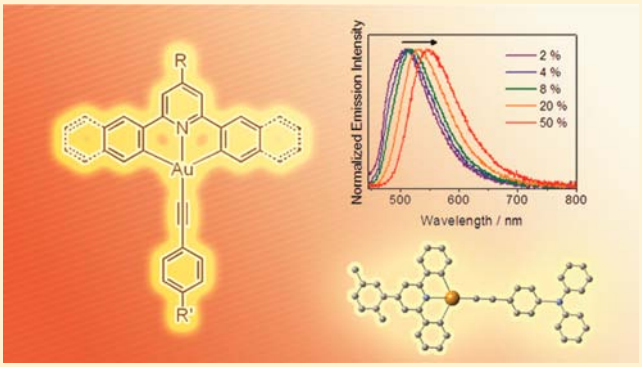

INTRODUCTION

There has been a rapid growth in the development of gold chemistry over the past few decades.[1−6] However, the luminescence behavior of gold(III) compounds has remained rather underexplored despite extensive studies on the related luminescent d^{10} gold(I) and d^8 platinum(II) complexes.[7] On the other hand, there has been increasing attention toward the utilization of luminescent transition metal compounds as functional materials, particularly in organic light-emitting devices (OLEDs).[8−14] It is believed that the incorporation of transition metal complexes into the emissive layer (EML) of OLEDs would increase the spin−orbit coupling and facilitate the intersystem crossing from singlet to triplet excited states, such that both singlet and triplet excitons can be harvested to improve the internal quantum efficiency of OLEDs to unity.[8] A state-of-the-art example would be the system of [Ir(ppy)$_3$] (ppy = 2-phenylpyridine) and its derivatives, in which the use of the cyclometalating ppy ligand has provided a simple but effective strategy to readily tune the emission colors across the visible region by varying the nature of the cyclometalating ppy ligand.[8b] To date, a variety of transition metal phosphors have been employed as light-emitting materials for OLED applications, including complexes of iridium(III),[8b,c,9] platinum(II),[8a,10−12] osmium(II),[13] and ruthenium(II)[14] systems. However, phosphorescent materials based on alternative metal centers, for instance the gold(III) metal center, remained rather limited.

The lack of luminescence from gold(III) complexes probably stems from the presence of low-energy d−d ligand field (LF) states and the electrophilicity observed for the gold(III) metal center. In order to enhance their luminescence, one way would be to coordinate strong σ-donating ligands to the gold(III) metal center, as first demonstrated by Yam and co-workers on gold(III) aryl compounds with room temperature photoluminescence and good air-stability.[15] This concept has further been extended and demonstrated in cyclometalated gold(III) complexes with σ-donating alkynyl and *N*-heterocyclic carbene ligands, which were found to emit in various media at both ambient and low temperatures.[16,17] Very recently, the potentials as light-emitting materials in vacuum-deposited and solution-processable OLEDs of some of the bis-cyclometalated gold(III) alkynyl complexes have been demonstrated.[16b,e,f] In order to gain an in-depth understanding on the nature of the bis-cyclometalated alkynylgold(III) system, a systematic study has been performed to investigate the effect of variation of the nature of the bis-cyclometalating ligand on the luminescence properties of the

Received: July 24, 2013
Published: October 21, 2013

dx.doi.org/10.1021/ic4019212 | *Inorg. Chem.* 2013, 52, 12713−12725

Chart 1

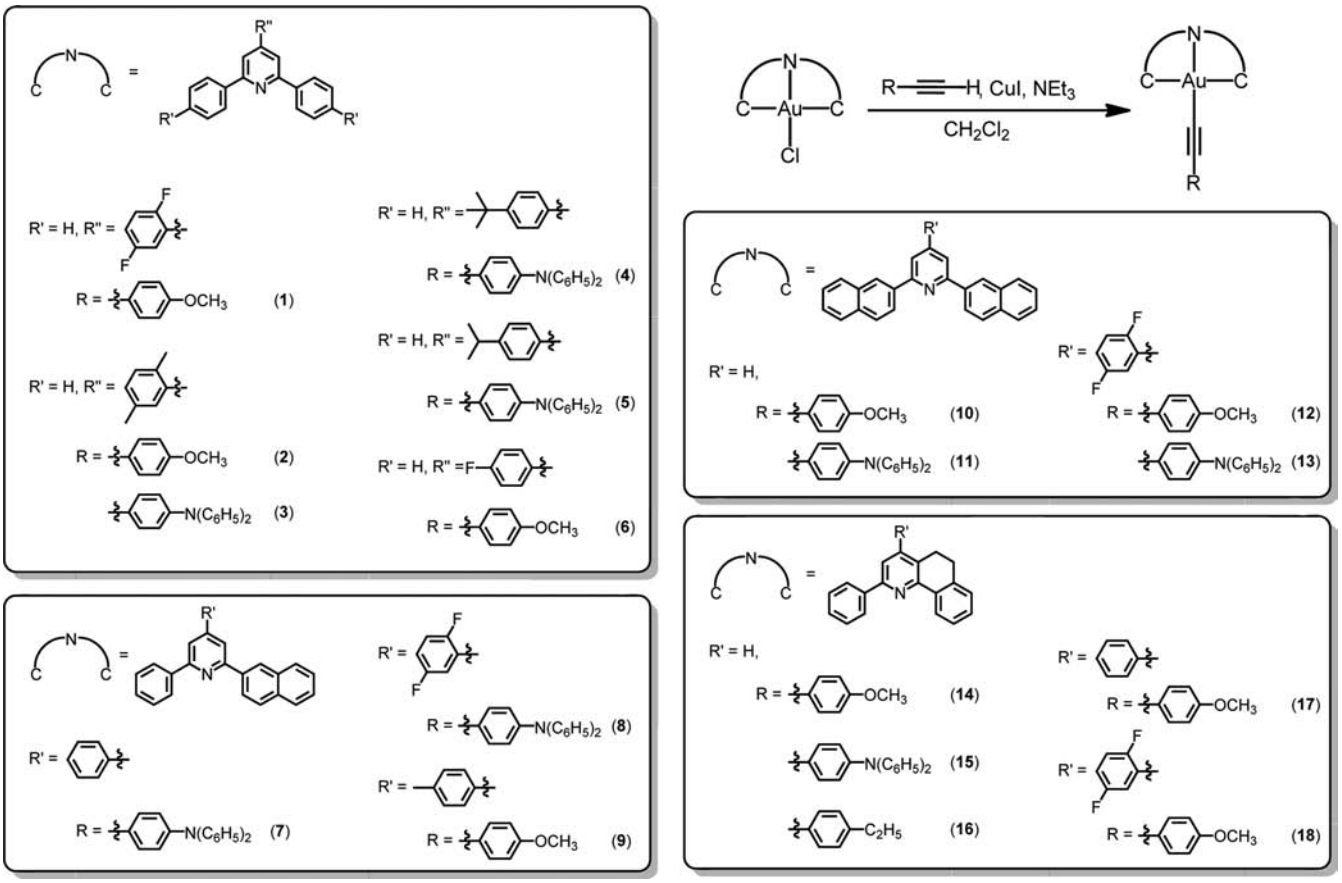

resulting gold(III) complexes. Herein, a comprehensive study of the synthesis, characterization, electrochemistry, photophysics, photochemistry, and electroluminescence of a series of bis-cyclometalated alkynylgold(III) complexes, [Au(R-C^N^C)-(C≡C—C_6H_4—R′)], is reported.

RESULTS AND DISCUSSION

Synthesis and Characterization. The gold(III) alkynyl complexes **1**−**18** (Chart 1) were synthesized according a modified literature procedure.[16a−c] A mixture of the chlorogold(III) precursor, [Au(R-C^N^C)Cl],[18] and the respective alkyne was stirred in dichloromethane in the presence of triethylamine and a catalytic amount of copper(I) iodide at room temperature under an inert atmosphere. The desired alkynylgold(III) complexes were isolated as yellow to orange-yellow crystals after purification by column chromatography on silica gel using dichloromethane as eluent, followed by subsequent recrystallization from slow diffusion of diethyl ether into the concentrated dichloromethane solution of the complex. All the complexes were soluble in dichloromethane and chloroform. In addition, good air- and thermal-stabilities have been observed. ^{1}H NMR spectroscopy and FAB-mass spectrometry have been performed to confirm the identities of the gold(III) complexes. Satisfactory elemental analyses have also been obtained. The complexes were found to exhibit a ν(C≡C) absorption at 2127−2157 cm^{-1} in the IR spectra, typical of terminal alkynyl coordination.

X-ray Crystal Structures. Single crystals of **1** and **6** were obtained by diffusion of diethyl ether vapor into a concentrated dichloromethane solution of the respective complex, and their crystal structures were determined by X-ray crystallography. Crystal structure determination data are summarized in Table 1. The selected bond distances and bond angles as well as selected intermolecular parameters are tabulated in Table 2. The perspective views of the crystal structures of **1** and **6** are depicted in Figure 1. All complexes showed square-planar geometries with slight distortions from the ideal arrangement in the crystal structures. The C−Au−N angles were in the range 80.66(18)−81.41(10)°, resulting from the steric requirements of the tridentate R-C^N^C ligands. The [Au(R-C^N^C)] moiety was generally in a coplanar conformation, with Au−C and Au−N bond distances of 2.054(3)−2.074(5) Å and 1.996(4)−2.001(2) Å, respectively. The Au—C≡C and C≡C—C angles of 171.5(3)−176.1(5)° and 175.3(6)−178.4(6)° were found to deviate slightly from the ideal linear geometry with bond angle of 180°. The Au—C and C≡C bond distances were found to be 1.953(3)−2.030(6) and 1.081(7)−1.206(5) Å, respectively. Such findings were similar to those of related cyclometalated gold(III) complexes that were reported earlier.[16a−c]

In these alkynylgold(III) complexes, the dihedral angles between the [Au(R-C^N^C)] plane and the plane of the phenyl ring of the aryl alkynyl ligand were in the range 15.848(88)−69.268(66)°. Complexes **1** and **6** exhibited π−π stacking interactions between adjacent [Au(R-C^N^C)] moieties arranged in a head-to-tail conformation with some π−π stacking interactions among the [Au(R-C^N^C)] planes, as revealed by an interplanar separation of 3.5177 and 3.4739 Å, respectively, between adjacent [Au(R-C^N^C)] planes. As in other related organogold(III) complexes,[16,17] the shortest Au···Au distances between adjacent molecules in complexes **1** and **6** of 5.7425(9) and 5.4988(3) Å, respectively, were found to be longer than the

dx.doi.org/10.1021/ic4019212 | Inorg. Chem. 2013, 52, 12713−12725

Table 1. Crystal and Structure Determination Data of Complexes 1 and 6

	[Au{C^N(2,5-$F_2C_6H_3$)^C}(C≡C—C_6H_4—OCH_3-*p*)] (**1**)	[Au{C^N(4-FC_6H_4)^C}(C≡C—C_6H_4—OCH_3-*p*)] (**6**)
empirical formula	$C_{32}H_{20}AuF_2NO$	$C_{32}H_{21}AuFNO$
fw	669.46	651.46
temp, K	301(2)	296(2)
wavelength, Å	0.710 73	0.710 73
cryst syst	monoclinic	triclinic
space group	$P2_1/n$	$P\bar{1}$
a, Å	10.474(2)	7.5267(2)
b, Å	14.057(3)	14.4607(4)
c, Å	16.738(3)	22.1759(6)
α, deg	90	92.502(2)
β, deg	97.82(2)	92.804(2)
γ, deg	90	100.828(1)
V, cm^3	2441.4(8)	2364.40(11)
Z, $Å^3$	4	4
density (calcd), g cm^{-3}	1.821	1.830
cryst size, mm^3	0.31 × 0.24 × 0.18	0.46 × 0.38 × 0.20
index ranges	$-9 \le h \le 12$	$-8 \le h \le 8$
	$-16 \le k \le 17$	$-17 \le k \le 16$
	$-20 \le l \le 19$	$-24 \le l \le 26$
reflections collected/unique	13 204/4631	39 085/8106
GOF on F^2	1.032	1.002
final *R* indices [$I > 2\sigma(I)$]	R1 = 0.0179	R1 = 0.0283
	wR2 = 0.0463	wR2 = 0.0561
largest diff peak and hole, e $Å^{-3}$	0.495 and −0.927	0.904 and −0.552

Table 2. Selected Bond Lengths (Å) and Angles (deg) for Complexes 1 and 6 with Estimated Standard Deviations (esd's) Given in Parentheses

[Au{C^N(2,5-$F_2C_6H_3$)^C}(C≡C—C_6H_4—OCH_3-*p*)] (**1**)		[Au{C^N(4-FC_6H_4)^C}(C≡C—C_6H_4—OCH_3-*p*)] (**6**)			
		Bond Lengths (Å)			
Au(1)−C(1)	1.953(3)	Au(1)−C(24)	1.982(6)	Au(2)−C(56)	2.030(6)
Au(1)−C(10)	2.054(3)	Au(1)−C(1)	2.064(5)	Au(2)−C(33)	2.070(5)
Au(1)−C(22)	2.067(3)	Au(1)−C(17)	2.063(5)	Au(2)−C(49)	2.074(5)
Au(1)−N(1)	2.001(2)	Au(1)−N(1)	1.996(4)	Au(2)−N(2)	1.996(4)
C(1)−C(2)	1.206(5)	C(24)−C(25)	1.135(7)	C(56)−C(57)	1.081(7)
		Bond Angles (deg)			
C(10)−Au(1)−C(22)	162.35(10)	C(1)−Au(1)−C(17)	161.4(2)	C(33)−Au(1)−C(49)	161.59(19)
N(1)−Au(1)−C(1)	175.90(11)	N(1)−Au(1)−C(24)	177.40(18)	N(2)−Au(2)−C(56)	179.33(18)
Au(1)−C(1)−C(2)	171.5(3)	Au(1)−C(24)−C(25)	175.6(5)	Au(2)−C(56)−C(57)	176.1(5)
N(1)−Au(1)−C(10)	81.41(10)	N(1)−Au(1)−C(1)	80.66(18)	N(2)−Au(2)−C(33)	80.85(17)
N(1)−Au(1)−C(22)	80.94(10)	N(1)−Au(1)−C(17)	80.80(18)	N(2)−Au(2)−C(49)	80.75(17)
C(1)−C(2)−C(3)	176.3(3)	C(24)−C(25)−C(26)	175.3(6)	C(56)−C(57)−C(58)	178.4(6)

sum of van der Waals radii for two gold(III) centers, revealing that no significant Au···Au interactions occurred in the crystal lattices of the complexes.

Electrochemistry. The electrochemical properties of the gold(III) alkynyl complexes, namely **1**−**18**, have been investigated by cyclic voltammetry in dichloromethane (0.1 mol dm^{-3} $^nBu_4NPF_6$). The complexes exhibited a reduction couple at −1.35 to −1.59 V, which was quasi-reversible versus saturated calomel electrode (SCE). An irreversible oxidation wave at +0.83 to +1.46 V versus SCE was also displayed (Table 3). Similar reduction potentials have generally been observed for complexes bearing the same R-C^N^C ligands. For instance, **2** and **3** with the same dimethylaryl-substituted C^N^C ligand were observed to show the same reduction potential at −1.50 V versus SCE. The reduction couples were therefore ascribed to the R-C^N^C ligand-centered reduction.[16] A less negative reduction potential has been observed upon the extension of *π*-conjugation in the presence of an additional aryl moiety on the central pyridine ring of the R-C^N^C ligand. This has caused a stabilization of the *π** orbital, rendering the complexes easier to be reduced. On the other hand, no significant change in the reduction potentials has been observed for complexes bearing peripheral naphthyl groups on the tridentate R-C^N^C ligands.

For the irreversible oxidative waves, the potentials were found to be dependent on the alkynyl ligands. Complexes bearing the electron-rich 4-diphenylaminophenylacetylene ligand were found to display a less positive potential at +0.83 to +0.89 V versus SCE. With a less electron-rich alkynyl ligand, the potential generally became more positive, and the oxidation waves were found to be insensitive to the nature of the cyclometalating R-C^N^C ligand. In view of the sensitivity of the oxidative waves

dx.doi.org/10.1021/ic4019212 | Inorg. Chem. 2013, 52, 12713−12725

(a)

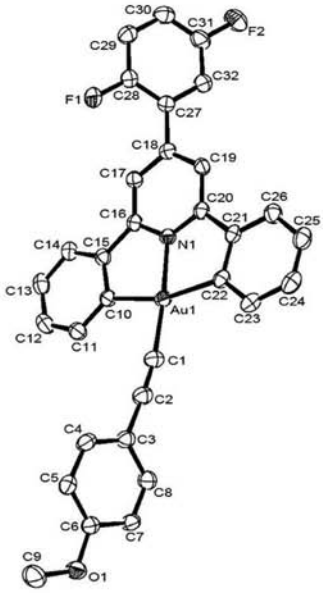

(b)

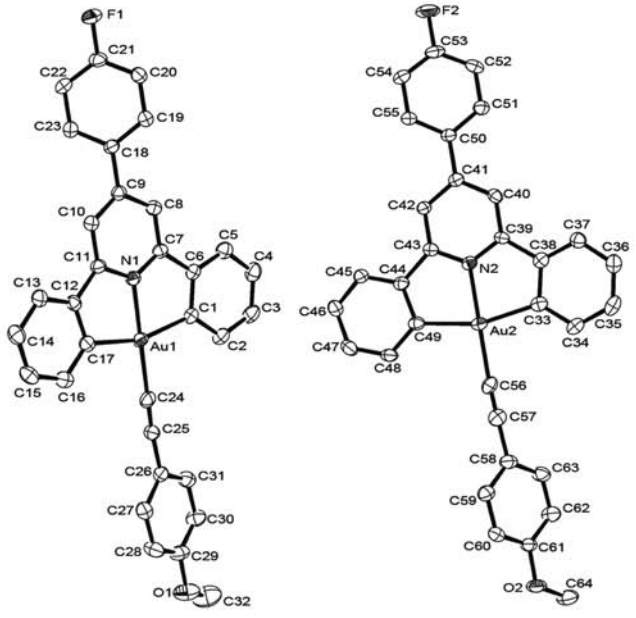

Figure 1. Perspective view of (a) **1** and (b) two independent molecules of **6** with atomic numbering scheme. Hydrogen atoms have been omitted for clarity. Thermal ellipsoids are drawn at the 30% probability level.

to the nature of the alkynyl moiety, the oxidation wave was assigned to an alkynyl-centered oxidation.

UV−Vis Absorption Spectroscopy. The UV−vis absorption spectra of complexes **1**−**18** in dichloromethane at 298 K generally featured an intense absorption band at *ca.* 302−332 nm and a moderately intense vibronic-structured band at 362−418 nm. For complexes containing aryl alkynyls substituted with the electron-rich diphenylamino moiety, an absorption shoulder was also observed toward the long wavelength end of the vibronic

Table 3. Electrochemical Data for 1−18[a]

complex	oxidation E_{pa}/V vs SCE[b]	reduction $E_{1/2}$/V vs SCE[c] (ΔE_p/mV)
1	+1.19	−1.35 (67)
2	+1.23	−1.50 (57)
3	+0.89	−1.50 (84)
4	+0.89	−1.47 (81)
5	+0.88	−1.47 (72)
6	+1.36	−1.44 (82)
7	+0.85	−1.44 (82)
8	+0.85	−1.35 (69)
9	+1.09	−1.46 (106)
10	+1.03	−1.55 (70)
11	+0.83	−1.53 (109)
12	+1.46	−1.36 (60)
13	+0.96	−1.34 (89)
14	+1.16	−1.59 (111)
15	+0.85	−1.58 (109)
16	+1.32	−1.57 (73)
17	+1.18	−1.54 (70)
18	+1.19	−1.45 (72)

[a]In dichloromethane solution with 0.1 M $^nBu_4NPF_6$ as supporting electrolyte at room temperature; working electrode, glassy carbon; scan rate 100 mV s^{-1}. [b]E_{pa} refers to the anodic peak potential for the irreversible oxidation waves. [c]$E_{1/2} = (E_{pa} + E_{pc})/2$; E_{pa} and E_{pc} are peak anodic and peak cathodic potentials, respectively. $\Delta E_p = |E_{pa} - E_{pc}|$.

band. The extinction coefficients (ε) were on the order of 10^3−10^4 dm^3 mol^{-1} cm^{-1}. These results were found to resemble those of other cyclometalated alkynylgold(III) complexes reported previously.[16] The photophysical data of **1**−**18** are summarized in Table 4 while the representative electronic absorption spectra of complexes **12**, **15**, and **18** are shown in Figure 2.

Considering the vibronic-structured band at 362−418 nm, comparison of complexes with the same cyclometalating ligand suggested that the absorption energy of this low-energy band showed negligible changes upon the variation of the terminal alkynyls. The vibrational progressional spacings of the low-energy band were found to lie between 1300 and 1400 cm^{-1}, which was in accordance to the skeletal vibrational frequencies of the tridentate ligand. The chloro precursor and other related alkynylgold(III) complexes were also found to exhibit similar absorption bands. With reference to the observations and literature results, the lower-energy band was assigned to a metal-perturbed π−π^* intraligand (IL) transition of the R-C^N^C ligand, with some charge-transfer character from the aryl moieties to the central pyridine moiety.[16] An assignment to a metal-to-ligand charge transfer (MLCT) transition would not be feasible due to the electrophilic and redox-inactive nature of the gold(III) metal center. For those complexes with electron-rich 4-diphenylaminophenylacetylene, the absorption shoulder beyond 400 nm would be assigned as a ligand-to-ligand charge transfer (LLCT) [π(C≡C—R) → π^*(R-C^N^C)] transition from the alkynyl moiety to the cyclometalating ligand.[16] Although the gold(III) metal center is a good electron acceptor and an assignment to a ligand-to-metal charge transfer (LMCT) has been proposed in other gold(III) complexes,[19] an assignment of the absorption bands to IL and LLCT transitions would be favored with reference to the computational studies of related alkynylgold(III) complexes[16c] and the good photostability of the present complexes since a LMCT transition would usually lead to photodecomposition of the gold(III) complexes.

dx.doi.org/10.1021/ic4019212 | *Inorg. Chem.* 2013, 52, 12713−12725

Table 4. Photophysical Data for 1−18

absorption[a] λ_{max}/nm (ε_{max}/dm^3 mol^{-1} cm^{-1})	emission medium (T/K)	λ_{max}/nm (τ_0/μs)	Φ_{em}[b]
Compound **1**			
308 (24 420), 332 (13 940), 386 (7550), 410 (5170)	CH_2Cl_2 (298)[c]	483, 518, 547 (0.1)	1×10^{-3}
	glass (77)[c,d]	474, 508, 544, 590sh (80)	
	thin film (298)		
	4% in PMMA	486, 515, 544	
Compound **2**			
312 (21 950), 362 (7760), 380 (7310), 400 (4800)	CH_2Cl_2 (298)[c]	476, 506, 542 (<0.1)	3×10^{-3}
	glass (77)[c,d]	470, 504, 529, 570sh (97)	
	thin film (298)		
	4% in PMMA	472, 502, 543	
Compound **3**			
314 (50 680), 384 (17 910), 400 (18 320)	CH_2Cl_2 (298)[c]	626 (<0.1)	0.01
	glass (77)[c,d]	471, 505, 542sh (441)	
	solid (298)	558 (<0.1)	
	solid (77)	555 (<0.1)	
	thin film (298)		
	2% in PMMA	520	
	4% in PMMA	525	
	8% in PMMA	527	
	20% in PMMA	534	
	50% in PMMA	554	
	2% in MCP	513	0.30
	4% in MCP	517	0.35
	8% in MCP	520	0.38
	20% in MCP	532	0.31
	50% in MCP	547	0.17
Compound **4**			
314 (64 630), 390 (12 600), 406 (13 060)	CH_2Cl_2 (298)[b]	629 (<0.1)	5×10^{-3}
	glass (77)[b,c]	472, 509, 555sh (273)	
	solid (298)	560 (<0.1)	
	solid (77)	557 (5.6)	
	thin film (298)		
	4% in PMMA	544	
	4% in MCP	522	0.44
Compound **5**			
314 (68 560), 390 (12 340), 404 (12 920)	CH_2Cl_2 (298)[b]	636 (3.6)	0.01
	glass (77)[b,c]	471, 505, 550sh (305)	
	solid (298)	565 (<0.1)	
	solid (77)	554 (8.8)	
	thin film (298)		
	4% in PMMA	529	
	4% in MCP	512	0.36
Compound **6**			
366 (6800), 382 (6460), 406 (4250)	CH_2Cl_2 (298)[c]	478, 510, 543sh (0.3)	2×10^{-3}
	glass (77)[c,d]	470, 504, 536 (114)	
Compound **7**			
308 (66 620), 380 (16 390), 400 (17 920)	CH_2Cl_2 (298)[c]	639 (0.2)	0.01
	glass (77)[c,d]	512, 562, 609, 668sh (2511)	
	thin film (298)		
	4% in PMMA	563	
	4% in MCP	562	0.22
Compound **8**			
312 (62 440), 384 (16 440), 402 (18 110)	CH_2Cl_2 (298)[c]	664 (0.1)	$<1 \times 10^{-3}$
	glass (77)[c,d]	500, 537, 582, 623sh (3374)	
	thin film (298)		
	4% in PMMA	572	
	4% in MCP	566	0.28
Compound **9**			
312 (47 830), 380 (12 880), 396 (12 070)	CH_2Cl_2 (298)[c]	562, 604, 663sh (25)	0.09
	glass (77)[c,d]	560, 604, 659sh (2285)	
	thin film (298)		
	4% in PMMA	560, 604, 663sh	
Compound **10**			
302 (66 980), 374 (29 780), 394 (37 500)	CH_2Cl_2 (298)[c]	559, 602, 657sh (64)	0.08
	glass (77)[c,d]	471, 503, 542 (262)	
Compound **11**			
302 (68 850), 376 (26 900), 394 (32 650)	CH_2Cl_2 (298)[c]	605 (4.8)	3×10^{-3}
	glass (77)[c,d]	515, 553, 597, 651sh (2876)	
Compound **12**			
304 (49 610), 386 (17 600), 406 (22 000)	CH_2Cl_2 (298)[c]	566, 607, 669sh (46)	0.01
	glass (77)[c,d]	500, 539, 579, 630sh (6622)	
Compound **13**			
322 (53 200), 388 (20 410), 406 (24 210)	CH_2Cl_2 (298)[c]	660 (<0.1)	1×10^{-3}
	glass (77)[c,d]	516, 574, 619, 677sh (252)	
	thin film (298)		
	4% in PMMA	569	
Compound **14**			
316 (15 080), 330 (12 640), 374 (6720), 394 (7370), 414 (6220)	CH_2Cl_2 (298)[c]	491, 525, 563sh (0.4)	1×10^{-3}
	glass (77)[c,d]	486, 522, 558, 609sh (178)	
	thin film (298)		
	4% in PMMA	495, 542, 583sh	
Compound **15**			
318 (33 850), 377 (11 150), 393 (13 760), 414 (11 850)	CH_2Cl_2 (298)[c]	612 (0.1)	6×10^{-3}
	glass (77)[c,d]	485, 524, 566sh (193)	
	thin film (298)		
	4% in PMMA	495, 542, 580sh	
Compound **16**			
316 (13 950), 375 (4550), 393 (5800), 415 (5370)	CH_2Cl_2 (298)[c]	493, 536, 583, 643sh (0.6)	4×10^{-3}
	glass (77)[c,d]	485, 522, 559 (211)	
	thin film (298)		
	4% in PMMA	492, 542, 583, 611	
Compound **17**			
316 (17 290), 334 (13 160), 374 (7230), 392 (7540), 414 (6120)	CH_2Cl_2 (298)[c]	490, 522, 558sh, 593sh (0.4)	$<1 \times 10^{-3}$
	glass (77)[c,d]	486, 513, 554, 596 (161)	
	thin film (298)		
	4% in PMMA	494, 542, 579	
Compound **18**			
318 (17 120), 336 (12 780), 378 (7470), 396 (8100), 418 (6470),	CH_2Cl_2 (298)[c]	496, 526, 565sh (0.4)	2×10^{-3}
	glass (77)[c,d]	489, 525, 558, 600 (164)	
	thin film (298)		
	4% in PMMA	497, 526	

[a]In dichloromethane at 298 K. [b]For CH_2Cl_2 solutions, the luminescence quantum yield, measured at room temperature using quinine sulfate as a standard; for thin films, the absolute photoluminescence quantum yield, measured under an excitation wavelength of 350 nm and at room temperature. [c]Vibronic-structured emission band. [d]In EtOH−MeOH−CH_2Cl_2 (40:10:1 v/v).

Comparison with related compounds containing the unsubstituted 2,6-diphenylpyridine (C^N^C) ligand[16a−c] suggested that the attachment of an additional aryl group to the central pyridine ring would result in a red shift in absorption energies, as in complexes **1**−**6**. The effects of different substituted aryl rings on the central pyridine ring of the tridentate ligand were rather

dx.doi.org/10.1021/ic4019212 | Inorg. Chem. 2013, 52, 12713−12725

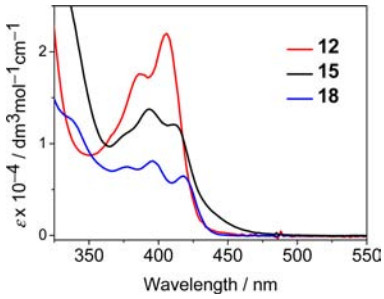

Figure 2. Electronic absorption spectra of complexes **12**, **15**, and **18** in dichloromethane at 298 K.

similar. The additional aryl moiety on the pyridine ring could stabilize the π^* orbital by better delocalization over the R-C^N^C ligand, giving rise to a narrowing of the $\pi-\pi^*$ energy gap and therefore a red shift in absorption. Attachment to different alkynyl moieties did not show any appreciable changes in the absorption energies, except that the presence of the electron-rich diphenylamino substituent on the aryl alkynyl would lead to an absorption tail extending up to 500 nm for the LLCT $\pi[C{\equiv}C{-}C_6H_4{-}N(C_6H_5)_2] \rightarrow \pi^*$(R-C^N^C) transition. Changing the phenyl moieties on the C^N^C ligand to the more-conjugated 2-naphthyl moieties could also lead to a red shift in absorption maxima of the complexes, as shown in **7**–**9** with one 2-naphthyl group and **10**–**14** with two 2-naphthyl groups. The use of the more conjugated naphthyl moieties in 2,6-di-2-naphthylpyridine has resulted in a destabilization of the HOMO π orbital and a stabilization of the LUMO π^* orbital, which led to a smaller HOMO–LUMO energy gap and gave rise to the red shifts in absorption. Comparison with complexes **1**–**6** demonstrated that increasing conjugation by the replacement of phenyl with 2-naphthyl groups (as in **10** and **11**) would cause a less pronounced red shift than by just lowering the LUMO π^* orbital with an additional aryl ring on the pyridine unit. Yet, the two effects could also be combined to synergistically cause a further red shift in the absorption energies to 386–406 nm as in complexes **12** and **13**. In addition, the presence of more conjugated naphthyl moieties has enhanced the absorption of the complexes as reflected by the higher extinction coefficients in **10**–**13**.

On the other hand, the use of the 5,6-dihydro-2,4-diphenylbenzo[*h*]quinoline (dhpbzq) ligand and its derivatives in **14**–**18** gave rise to a red shift in absorption wavelength to 374–418 nm, compared to the unsubstituted 2,6-diphenylpyridine ligand.[16a–c] The dhpbzq ligand featured an ethylidene bridge that would fix the phenyl ring near the molecular plane and would probably influence the electronic states of the cyclometalating ligand. In addition, the dhpbzq ligand could be regarded as a C^N^C ligand with electron-donating $-CH_2CH_2-$ substituents on one of the aryl rings in *ortho*-position as well as on the *meta*-position of the pyridine ring. As the electronic effect is more dominating at the *ortho*-position on the aryl ring than at the *meta*-position on the pyridine ring, this would probably result in a destabilization of the frontier orbitals, eventually causing the HOMO–LUMO gap to be diminished and thus a red shift in absorption.

Luminescence Spectroscopy. This class of organogold(III) compounds was found to exhibit strong luminescence. Their photoluminescence properties in various media at ambient and low temperatures have been studied. All alkynylgold(III) complexes were observed to exhibit rich luminescence behaviors, spanning through the visible region from 451 to 669 nm (photoexcitation at wavelengths ≥330 nm). The photophysical data are summarized in Table 4. The representative solution emission spectra of complexes **12**, **15**, and **18** are shown in Figure 3.

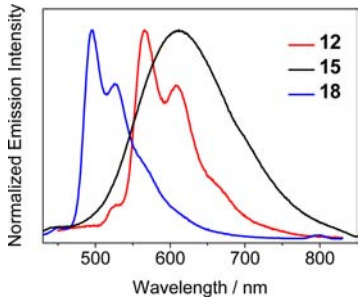

Figure 3. Normalized emission spectra of complexes **12**, **15**, and **18** in dichloromethane at 298 K.

Previous studies have suggested that the emission properties of this class of alkynylgold(III) complexes were rather insensitive to the nature of the alkynyl ligand.[16a–c] However, with the incorporation of electron-rich amino substituents on the alkynyl moiety, a change in the emission origin was observed, and thus the emission properties are different.[16a–c] With the aim to fine-tune the emission energies of the alkynylgold(III) complexes, efforts have been put into the preparation of alkynylgold(III) complexes with a variety of cyclometalating C^N^C ligands. It was anticipated that variation of the substituents on the C^N^C ligands could adjust the energy levels of the frontier orbitals of the complexes, thereby giving rise to a series of alkynylgold(III) complexes with different emission properties. In order to better compare the change in luminescence behaviors as a function of the cyclometalating ligands, the ancillary alkynyl ligands have been fixed as 4-methoxyphenylacetylene and 4-diphenylaminophenylacetylene in most of the cases.

Upon excitation at $\lambda \geq 350$ nm in dichloromethane solution at 298 K, complexes containing the 4-methoxyphenylalkynyl ligand, namely complexes **1**, **2**, **6**, **9**, **10**, **12**, **14**, **17**, and **18**, as well as complex **16** which contained the 4-ethylphenylalkynyl ligand, were found to exhibit similar vibronically structured emission bands, with emission maxima at *ca.* 476–669 nm. Complexes bearing identical tridentate ligands showed emission maxima at essentially the same wavelengths, confirming the insensitivity of the emission energies to the nature of the alkynyl ligands. The vibrational progressional spacings were *ca.* 1300–1400 cm^{-1}, which were characteristic of the stretching frequencies of the C=C and C=N bonds in the pincer ligands, indicating that the excited state might involve the participation of the cyclometalating ligand. According to the assignment of similar bands in related gold(III) complexes,[16a–c] the emission of these alkynylgold(III) complexes were assigned as originating from a metal-perturbed triplet IL $^3[\pi \rightarrow \pi^*$ (R-C^N^C)] state, with some aryl-to-pyridine charge-transfer character.

A detailed investigation into these vibronically structured emission bands could reflect how the variation of the cyclometalating R-C^N^C ligands would affect the emission properties of the complexes. Similar to the UV–vis absorption study, the attachment of an additional aryl moiety to the central pyridine ring of the bis-cyclometalating ligand has led to a red shift in emission, as shown in complexes **1**, **2**, and **6** (λ_{em} = 478–483 nm). Upon the attachment of the aryl substituent, better delocalization would result in the stabilization of the pyridine-based LUMO π^* orbital, and therefore a smaller $\pi-\pi^*$ energy

dx.doi.org/10.1021/ic4019212 | *Inorg. Chem.* 2013, 52, 12713–12725

gap. Attempts to use more conjugated R-C^N^C ligands by the replacement of phenyl rings with 2-naphthyl moieties have resulted in further red shifts in the emission maxima. In particular, complex **12**, with an additional difluoroaryl moiety attached on the pyridine ring, exhibited an emission down to 566 nm. The presence of naphthyl units would lead to more extended electron delocalization in the tridentate ligand. This would probably destabilize the HOMO π orbital, resulting in a narrowing of the $\pi-\pi^*$ energy gap to cause a red shift in the emission maximum.

For complexes **14**, **16**, **17**, and **18** that contained 5,6-dihydro-2-phenyl-benzo[*h*]quinoline (dhpbzq) derivatives as the R-C^N^C ligand, the emission maxima were found to be at 490–496 nm, and the emission band could be assigned to a metal-perturbed IL $^3[\pi \rightarrow \pi^*$ (R-C^N^C)] origin. The red shift in emission compared to complexes **1**, **2**, and **6** could be attributed to the fixing of the phenyl ring near the molecular plane of the tridentate ligand by the $-CH_2CH_2-$ bridging group that caused further planarization of the molecule as well as the additional electron-donating effect of the linkage, and hence a narrower HOMO–LUMO energy gap would result. Similarly, the presence of an additional aryl ring on the pyridine moiety in **17** and **18** would give rise to a further reduction in the emission energy.

For complexes containing the electron-rich 4-diphenylamino-phenylacetylene ligand, i.e., complexes **3**, **4**, **5**, **7**, **8**, **11**, **13**, and **15**, their solution emission spectra featured a broad, structureless, low-energy emission band at 605–669 nm. These emission bands were found to be independent of the concentration of the sample solution in the range 2×10^{-6} to 3×10^{-3} mol dm^{-3}, so it would be impossible to assign the emission as excimeric bands resulting from the $\pi-\pi$ stacking of the R-C^N^C planes. With reference to previous studies,[16a−c] these low-energy emission bands were assigned as originating from a ^{3}LLCT [π(C≡C—C_6H_4—N(C_6H_5)$_2$-*p*) → π^*(R-C^N^C)] excited state.

A detailed comparison could be made between the above results and that of a literature compound, [Au(C^N^C)(C≡C—C_6H_4—N(C_6H_5)$_2$-*p*)], which exhibited an emission maximum at 620 nm in dichloromethane at 298 K.[16a−c] Generally speaking, complexes **3**, **4**, **5**, **7**, **8**, and **13**, with an additional aryl moiety on the pyridine group of the tridentate ligand, exhibited emission maxima at lower energies, since the aryl substituent would increase the conjugation on the tridentate ligand and would make the LUMO π^* orbital of the tridentate ligand, which contained predominantly pyridine character, more lower-lying in energy. As a result, the HOMO–LUMO gap for the LLCT transition is smaller, and a red shift occurs. Complex **15** was found to show a blue shift in emission relative to the literature complex with unsubstituted C^N^C ligand, probably due to the destabilization of the LUMO π^* orbital caused by the dhpbzq ligand as discussed above. On the other hand, the presence of two naphthyl moieties in complex **11** failed to cause a red shift in the emission maximum. It was expected that the increase in the extent of conjugation should lead to a stabilization of the π^* orbital of the C_{Np}^N^C_{Np} ligand, and with a lower-lying LUMO π^* orbital, the emission coming from the LLCT origin should be of lower energy. However, complex **11** exhibited a higher-energy emission at 605 nm. Comparison of the emission of **8** and **13** also gave the same increase in emission energies with increasing number of naphthyl moieties. In fact, electrochemical studies (*vide supra*) revealed that the energies of the LUMO π^* orbitals are quite close-lying in nature, as shown by their similar reduction potentials. However, complexes with C_{Np}^N^C_{Np} ligands were found to show slightly more negative reduction potentials than those with C^N^C ligands, indicating that the LUMO π^* orbital is actually slightly more higher-lying in nature. A probable reason might be that the increased conjugation by the naphthyl moieties would cause an increase in electron density of the π^* orbital of the R-C^N^C ligand, and the limited rotation of naphthyl groups would also exert a significant influence on the electronic states of the cyclometalating ligand. This would slightly destabilize the pyridine-based LUMO π^* orbital and cause a higher-energy emission coming from the LLCT excited state.

Upon excitiation at $\lambda \geq 350$ nm, the emission spectra in alcoholic glass at 77 K of the complexes were found to exhibit vibronically structured bands with maxima ranging from 470 to 567 nm, similar to those observed in dichloromethane solution. These vibronically structured emission bands were assigned to originate from a metal-perturbed ^{3}IL [$\pi \rightarrow \pi^*$(R-C^N^C)] excited state. It is remarkable that those complexes showing structureless ^{3}LLCT emissions in fluid solutions all exhibited similar vibronically structured emission bands in low-temperature glasses, associated with a change in emission origin from ^{3}LLCT [π(C≡C—C_6H_4—R) → π^*(R-C^N^C)] excited states to ^{3}IL [$\pi \rightarrow \pi^*$(R-C^N^C)] excited states. These observations at reduced temperatures suggested that these ^{3}LLCT and ^{3}IL excited states were of similar energies. The presence of naphthyl groups was observed to cause a dramatic increase in the glass emission lifetime with an increase in conjugation, indicating the substantial mixing of the ^{3}IL character into the emissive state. The representative emission spectra of complexes **12**, **15**, and **18** in low-temperature glass are shown in Figure 4.

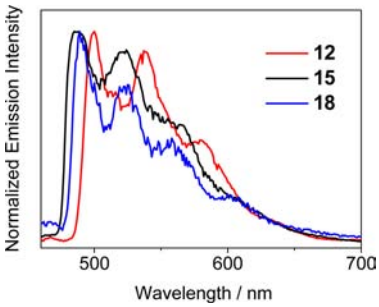

Figure 4. Normalized emission spectra of complexes **12**, **15**, and **18** in EtOH–MeOH–CH_2Cl_2 (40:10:1 v/v) glass at 77 K.

The emission spectra of selected complexes were also measured in the solid state or in solid-state thin films. At low dopant concentration of 4 wt % in polymethylmethacrylate (PMMA), the complexes generally exhibited emission that resembled the solution emission. In particular, complex **3** was selected for concentration-dependent solid-state thin film emission studies (see Figure 5a). The complexes displayed similar low-energy structureless emission bands with a shift in emission energies from 520 to 554 nm in the concentration range 2–50 wt % when doped in PMMA at 298 K. In the solid state, the emission energy was further shifted to 558 nm. The same trend was also observed when complex **3** was doped into a wide bandgap host material, *N*,*N*′-dicarbazolyl-3,5-benzene (MCP). As shown in Figure 5b, a red shift of 1326 cm^{-1} in emission energies was found upon increasing the concentration of **3** in MCP from 2 to 50 wt %. The observation of such concentration-dependent emission was likely to arise from the excimeric emission caused by the $\pi-\pi$ stacking interactions of the

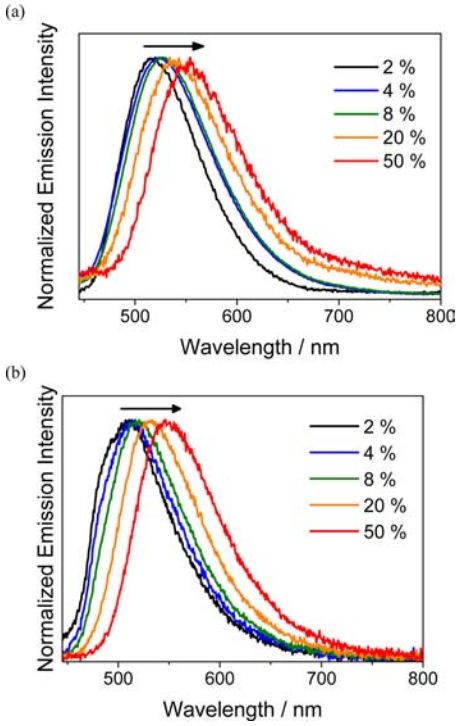

Figure 5. Normalized emission spectra of the thin films of **3** doped in (a) PMMA and (b) MCP at different concentrations at 298 K.

R-C^N^C moieties with higher order and better packing of molecules at increased concentrations, as supported by the occurrence of $\pi-\pi$ stacking in the crystal packing of the complexes.

The absolute photoluminescence quantum yields (PLQYs) of selected complexes **3**, **4**, **5**, 7, and **8** in solid-state thin films were also measured. A high PLQY ranging from 22 to 44% was obtained in 4 wt % doped thin films. In particular, the PLQY of complex **4** in thin film was 4 orders of magnitude higher than that in solution. The corresponding intramolecular motions and relatively free rotations of molecules in solution may be the origin of weak phosphorescence, leading to a low PLQY. Table 4 lists the absolute PLQY of the selected complexes at a concentration of 4 wt % doped into MCP thin films under an excitation wavelength of 350 nm.

Transient Absorption Studies. The excited state species is regarded as a different chemical species from the corresponding ground state species. In order to obtain more information on the nature of the excited states, nanosecond transient absorption (TA) measurements were performed on complexes **3** and **15**–**17** in degassed dichloromethane solution at room temperature. The TA difference spectra of complexes **15**–**17** determined at different delay times after a 355-nm laser pulse excitation and the respective decay traces are shown in Figure 6.

Complex **3** was observed to show a negative absorption band at 385 nm corresponding to ground-state bleaching, a weak positive band at 445 nm, as well as a moderately intense, broad positive band at 688 nm with a decay lifetime of 21.9 μs. The bleaching was ascribed to the depletion of ground state species, leading to the diminution of the intraligand $\pi-\pi^*$ transition of the R-C^N^C ligand. In light of the longer decay lifetime of the transient signals than that of the emission decay, it was possible that a charge-separated excited state had formed. The higher energy TA band at 445 nm could tentatively be assigned to be originated from the radical anion of the R-C^N^C ligand, on the basis of a literature report on Ir(III) complexes containing the

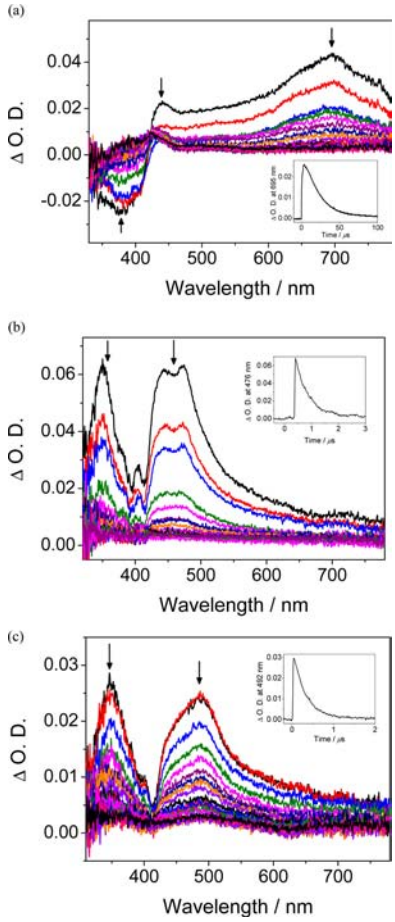

Figure 6. (a) Transient absorption difference spectra of **15** in CH_2Cl_2 at room temperature at decay times of 0–100 μs with time intervals of 5 μs. Inset shows the decay trace of the absorptions monitored at 695 nm. (b) Transient absorption difference spectra of **16** in CH_2Cl_2 at room temperature at decay times of 0–3 μs with time intervals of 0.2 μs. Inset shows the decay trace of the absorptions monitored at 492 nm. (c) Transient absorption difference spectra of **17** in CH_2Cl_2 at room temperature at decay times of 0–1 μs with time intervals of 50 ns. Inset shows the decay trace of the absorptions monitored at 492 nm.

related cyclometalating 2-phenylpyridine (ppy) ligand.[20] On the other hand, the lower energy, broad TA band could tentatively be assigned as the radical cation absorption of the electron-rich 4-diphenylaminophenylacetylene moiety. A similarly broad TA band could be observed in the absorption spectra of the related triphenylamine radical cation at 550–680 nm,[21–24] and similar bands were also exhibited by the radical cations of the related 4-aminophenylalkynyl molecule.[24] Similarly, complex **15** was observed to exhibit a ground state bleaching signal at 375 nm, a higher energy TA band at 440 nm, which was tentatively assigned as the absorption of the radical anion of the tridentate ligand, as well as a lower energy broad TA band at 695 nm assignable to the absorption of the radical cation of 4-diphenylaminophenylacetylene. The decay lifetime was found to be 24.6 μs.

On the other hand, for complexes **16** and **17**, no ground state bleaching was observed, but absorption bands could be seen at *ca.* 348 and 444–487 nm, with a decay lifetime of 0.5 and 0.3 μs, respectively. The TA decay lifetimes in each case were found to be comparable to those of the emission decay lifetimes of the complexes in dichloromethane, which supported the assignment of a transient absorption derived from the $^3\pi,\pi^*$ excited state of the complexes.

dx.doi.org/10.1021/ic4019212 | *Inorg. Chem.* 2013, 52, 12713–12725

Electroluminescence Properties. The recent developments of phosphorescent emitters for organic light-emitting devices based on organometallic complexes have been directed toward the use of iridium(III), platinum(II), and other metal centers, while related studies on the gold(III) metal complexes have been very limited. Since the synthesis of luminescent gold(III) complexes was demonstrated to be successful, and their photophysical properties and emission colors could be fine-tuned by modulating the cyclometalating ligands or the ancillary alkynyls, the gold(III) complexes were expected to be attractive candidates for OLED applications. Previous studies by the group of Yam have demonstrated that an OLED device based on luminescent gold(III) complexes could achieve high current efficiency and external quantum efficiency (EQE).[16b,e,f] It would be interesting to extend this work and hopefully to further improve the performance of such OLED devices.

Multilayer OLEDs with the structures of indium−tin oxide (ITO)/α-naphthylphenylbiphenyldiamine (NPB) (70 nm)/4,4′,4″-tris(carbazole-9-yl)-triphenylamine (TCTA) (5 nm)/x% Au(III) complex:4,4′-bis(carbazol-9-yl)biphenyl (CBP) (30 nm)/bis(2-methyl-8-quinolinato)-4-phenylphenolate) aluminum(III) (BAlq) (30 nm)/LiF (0.8 nm)/Al had been prepared by thermal evaporation, in which selected complexes **3** and **4** were chosen as phosphorescent dopants doped into MCP host material at different concentrations (x) of 2%, 4%, 6%, and 8%. NPB and BAlq were used as hole-transporting and electron-transporting layers, respectively; while TCTA was employed as carrier confinement layer. Figure 7 depicts the electroluminescence (EL) spectra of devices doped with **3** as phosphorescent dopant at a current density of 100 mA cm^{-2}. The devices exhibited a broad, structureless emission band. The EL spectra are in accordance with their photoluminescence spectra in solid-state thin films, thus confirming that they originate from the same ^{3}LLCT [π(C≡C—C_6H_4—N(C_6H_5)$_2$-p) → π*(R-C^N^C)] excited state of the cyclometalating ligand. In addition, the EL peak maxima were found to shift from 502 to 514 nm with increasing dopant concentration from 2% to 8%, while the Commission Internationale de L'Eclairage (CIE) coordinates were found to shift from (0.23, 0.41) to (0.24, 0.48), in good agreement with the emission spectra in the doped thin films. Similar concentration-dependent behavior was also observed for devices doped with complex **4**. The concentration dependence might be ascribed to the excimeric emission resulting from π-stacking of the cyclometalating ligand and a better packing of molecules at higher concentrations, which is well-documented in square-planar metal complexes. Devices doped with complexes **3** and **4** demonstrate promising performance with high current efficiencies of 15.0 and 11.4 cd A^{-1} and EQE of 4.8% and 3.6%, respectively. The device performance of the devices doped with complex **3** is depicted in Figure 8 while the EL spectra and device

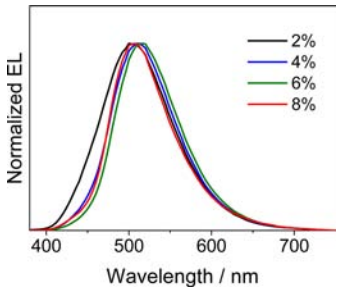

Figure 7. Normalized EL spectra of devices doped with **3** as phosphorescent dopant at a current density of 100 mA cm^{-2}.

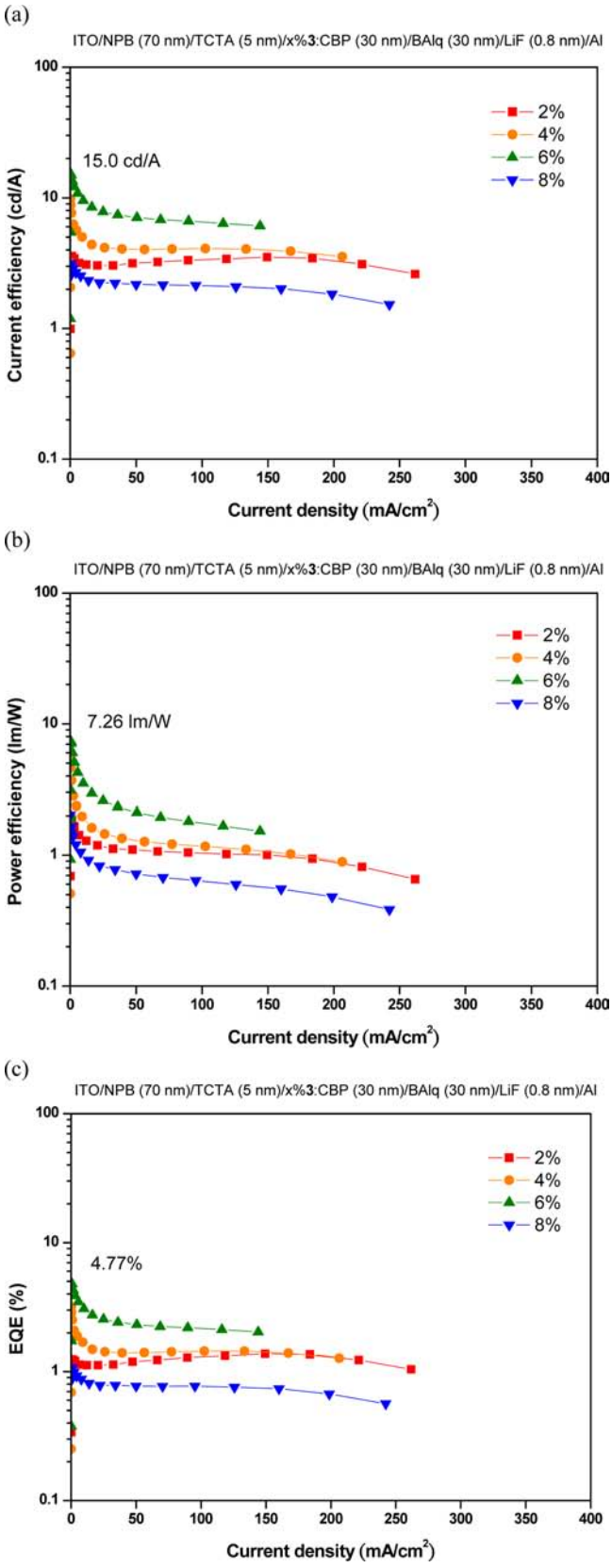

Figure 8. (a) Current and (b) power efficiencies and (c) external quantum efficiencies (EQE) of the devices with different concentrations of **3** doped into the CBP layer as a function of current density.

dx.doi.org/10.1021/ic4019212 | *Inorg. Chem.* 2013, 52, 12713−12725

performance for complex **4** are shown in Figure S1 in the Supporting Information. Further work on improvement of the OLED performance of these alkynylgold(III) complexes is currently in progress.

CONCLUSION

A comprehensive study has been performed on a novel class of luminescent alkynylgold(III) complexes containing various tridentate bis-cyclometalating ligands derived from 2,6-diphenylpyridine (R-C^N^C), [Au(R-C^N^C)(C≡C—C_6H_4—R′)]. The crystal structures of some of the complexes have been determined by X-ray crystallography. Electrochemical studies show a R-C^N^C ligand-centered reduction at −1.35 to −1.59 V versus SCE, as well as an alkynyl-centered oxidation at +0.83 to +1.46 V versus SCE. In dichloromethane solution at room temperature, the complexes generally showed a moderately intense vibronic-structured absorption band at 362−418 nm, assignable to the metal-perturbed $\pi-\pi^*$ IL transition of the R-C^N^C ligand. These alkynylgold(III) complexes were found to exhibit rich luminescence. Upon variation of the bis-cyclometalating and alkynyl ligands, the emission of the complexes could be tuned across the visible region from 476 to 669 nm in dichloromethane at room temperature. The complexes were also found to be emissive in low-temperature glass and in thin films at room temperature. Transient absorption studies have also been performed to investigate the excited state properties of selected complexes. In light of the rich luminescence behaviors of this class of gold(III) complexes, some of them have been employed in the EML of OLED devices and demonstrated interesting electroluminescence, in which the emission wavelengths were found to be red-shifted with increasing dopant concentration. In accordance with the emission spectra in the doped thin films, the concentration dependence is ascribed to the π-stacking of the cyclometalating R-C^N^C ligand. Promising device performance with high current efficiencies up to 15.0 cd A^{-1} and EQE of 4.8% could be achieved. It is proved that these alkynylgold(III) complexes are potential candidates for OLED materials.

EXPERIMENTAL SECTION

Materials and Reagents. $K[AuCl_4]$ was obtained from ChemPur. All chlorogold(III) precursors, [Au(R-C^N^C)Cl] (where R-C^N^C denotes any tridentate C^N^C-type cyclometalating ligands derived from 2,6-diphenylpyridine), were synthesized by transmetalation *via* the corresponding chloromercury(II) complex, [Hg(R-HC^N^C)Cl], according to a reported procedure.[18] All cyclometalating C^N^C-type ligands, R-HC^N^CH, were prepared from the respective acetophenones and benzaldehydes according to the well-documented procedure first reported by Kröhnke.[25] CuI was purchased from Lancaster, triethylamine and 2,6-diphenylpyridine were from Aldrich, while 4-methoxyphenylacetylene and 4-ethylphenylacetylene were from Acros. 4-Diphenylaminophenylacetylene was synthesized according to literature procedures.[26] Other solvents were purified and distilled using standard procedures prior to use. All other reagents were of analytical grade and used as received. All reactions were performed under anaerobic and anhydrous conditions using standard Schlenk techniques under an inert atmosphere of nitrogen unless otherwise specified.

Physical Measurements and Instrumentation. UV−vis spectra were obtained on a Hewlett-Packard 8452A diode array spectrophotometer. ^{1}H NMR spectra were recorded on a Bruker DPX-300 (300 MHz) or Bruker DPX-400 (400 MHz) Fourier transform NMR spectrometer with chemical shifts recorded relative to tetramethylsilane (Me_4Si). Positive FAB mass spectra were recorded on a Finnigan MAT95 mass spectrometer. Elemental analyses for the metal complexes were performed on the Carlo Erba 1106 elemental analyzer at the Institute of Chemistry, Chinese Academy of Sciences, in Beijing. Steady-state excitation and emission spectra were recorded on a Spex Fluorolog-2 model F111 fluorescence spectrofluorometer equipped with a Hamamatsu R-928 photomultiplier tube. Photophysical measurements in low-temperature glass were carried out with the sample solution loaded in a quartz tube inside a quartz-walled Dewar flask. Liquid nitrogen was placed into the Dewar flask for low temperature (77 K) photophysical measurements. Excited-state lifetimes of solution samples were measured using a conventional laser system. The excitation source used was the 355-nm output (third harmonic, 8 ns) of a Spectra-Physics Quanta-Ray Q-switched GCR-150 pulsed Nd:YAG laser (10 Hz). Luminescence quantum yields were measured by the optical dilute method reported by Demas and Crosby.[27] A degassed aqueous solution of quinine sulfate in 1.0 N sulfuric acid (Φ = 0.546, excitation wavelength at 365 nm) was used as the reference and corrected for the refractive index of the solution.[27b] All solution samples for photophysical studies were freshly prepared under a high vacuum in a 10-cm^3 round-bottomed flask equipped with a side arm 1-cm fluorescence cuvette and sealed from the atmosphere by a Rotaflo HP6/6 quick-release Teflon stopper. Solutions were rigorously degassed on a high-vacuum line in a two-compartment cell with no less than four successive freeze−pump−thaw cycles. Absolute luminescence quantum yields of thin films were measured on a Hamamatsu C9920-03 absolute PL quantum yield measurement system. Cyclic voltammetric measurements were performed by using a CH Instruments, Inc. model CHI 600A electrochemical analyzer. The electrolytic cell used was a conventional two-compartment cell. Electrochemical measurements were performed in dichloromethane solutions with 0.1 M ^{n}Bu_4NPF_6 as supporting electrolyte at room temperature. The reference electrode was a $Ag/AgNO_3$ (0.1 M in acetonitrile) electrode, and the working electrode was a glassy carbon electrode (CH Instruments, Inc.) with a platinum wire as the counter electrode. The working electrode surface was first polished with a 1-μm alumina slurry (Linde), followed by a 0.3-μm alumina slurry, on a microcloth (Buehler Co.). The ferrocenium/ferrocene couple ($FeCp_2^{+/0}$) was used as the internal reference.[28] All solutions for electrochemical studies were deaerated with prepurified argon gas just before measurements. Transient absorption measurements were performed on a LP920-KS laser flash photolysis spectrometer (Edinburgh Instruments Ltd., Livingston, U.K.) at ambient temperature. The excitation source was the 355-nm output (third harmonic) of a Nd:YAG laser (Spectra-Physics Quanta-Ray Lab-130 Pulsed Nd:YAG Laser), and the probe light source was a Xe900 450W xenon arc lamp. The transient absorption spectra were detected by an image intensified CCD camera (Andor) with PC plug-in controller, fully operated by L900 spectrometer software. The absorption kinetics were detected by a Hamamatsu R928 photomultiplier tube and recorded on a Tektronix model TDS3012B (100 MHz, 1.25 GS/s) digital oscilloscope and analyzed using the same software for exponential fit (tail-fit data analysis). All solutions for transient absorption measurements were degassed as in emission spectroscopic measurements.

Crystal Structure Determination. Single crystals of **1** and **6** suitable for X-ray diffraction studies were grown by vapor diffusion of diethyl ether into a concentrated dichloromethane solution of the complex. The X-ray diffraction data were collected on a Bruker Smart CCD 1000, using graphite monochromatized Mo-Kα radiation (λ = 0.710 73 Å). For complex **1**, raw frame data were integrated with *SAINT*[29] program, and semiempirical absorption correction with *SADABS*[30] was applied. The structures of all the complexes were solved by direct methods employing the SHELXS-97 program.[31] Full-matrix least-squares refinement on F^2 was used in the structure refinement. The positions of H atoms were calculated on the basis of the riding mode with thermal parameters equal to 1.2 times those of the associated C atoms and participated in the calculation of final *R*-indices. In the final stage of least-squares refinement, all non-hydrogen atoms were refined anisotropically.

OLED Fabrication and Characterization. The OLEDs were fabricated on patterned ITO-coated glass substrates with a sheet resisstance of 30 Ω/sq. The substrates were cleaned with Decon 90, rinsed with deionized water, dried in an oven, and treated in an ultraviolet ozone chamber. A 70-nm thick NPB was used as the hole-transporting layer, and a 5-nm thick TCTA was used as the carrier

dx.doi.org/10.1021/ic4019212 | *Inorg. Chem.* 2013, 52, 12713−12725

confinement layer. A 30-nm thick emissive layer consisting of 2%, 4%, 6%, and 8% selected complex was doped into the CBP layer *via* thermal codeposition. A 30-nm thick BAlq was used as the electron-transporting layer; while LiF/Al was used as metal cathode. All films were sequentially deposited at a rate of 0.1−0.2 nm s^{-1} without vacuum break. A shadow mask was used to define the cathode and to make four 0.1 cm^2 devices on each substrate. Current density−voltage−luminance (*J*−*V*−*L*) characteristics and EL spectra were measured simultaneously with a programmable Keithley 2420 power source and a Photoresearch PR-655 spectroradiometer.

Synthesis. *General Procedure for Syntheses of Alkynylgold(III) Complexes.* The alkynylgold(III) complexes were prepared according to a literature procedure. To a mixture of the gold(III) chloro precursor, [Au(R-C^N^C)Cl] (0.50 mmol), and a catalytic amount of copper(I) iodide (10 mg, 0.05 mmol) was added dichloromethane (35 mL). Triethylamine (2 mL) and the respective alkyne (0.75 mmol) were added to the resulting suspension. After stirring under an inert atmosphere at ambient temperature for 3 h, the solvent was removed *in vacuo*. The resulting residue was purified by column chromatography on silica gel with dichloromethane. The complex was then recrystallized by slowly diffusing diethyl ether vapor into the concentrated dichloromethane solution to give yellow solids.

*[Au{C^N(2,5-$F_2C_6H_3$)^C}(C≡C—C_6H_4—OCH_3-p)] (**1**).* HC^N(2,5-$F_2C_6H_3$)^CH = 2,6-diphenyl-4-(2,5-difluorophenyl)pyridine. This was synthesized from [Au{C^N(2,5-$F_2C_6H_3$)^C}Cl] (287 mg, 0.50 mmol) and 4-methoxyphenylacetylene (99 mg, 0.75 mmol). Complex **1** was obtained as yellow crystals. Yield: 100 mg (30%). ^{1}H NMR (300 MHz, $CDCl_3$, 298 K)/ppm: δ 3.84 (s, 3H, −OCH_3), 6.87 (d, 2H, *J* = 7.3 Hz, phenyl of C^N^C), 7.20 (m, 2H, −C≡CC_6H_4−), 7.33 (m, 2H, −C≡CC_6H_4−), 7.40 (m, 2H, phenyl of C^N^C), 7.53−7.61 (m, 6H, 2,5-$F_2C_6H_3$, phenyl and pyridine of C^N^C), 8.08 (d, 2H, *J* = 7.3 Hz, phenyl of C^N^C), 8.42 (d, 1H, 7.3 Hz, 2,5-$F_2C_6H_3$). Positive FAB-MS: *m*/*z* 670[M]$^+$. IR (KBr): 2157 cm^{-1} (ν(C≡C)). Anal. Calcd for $C_{32}H_{20}AuF_2NO$ (Found): C, 57.41 (57.58); H, 3.01 (2.88); N, 2.09 (2.17).

*[Au{C^N(2,5-$Me_2C_6H_3$)^C}(C≡C—C_6H_4—OCH_3-p)] (**2**).* HC^N(2,5-$Me_2C_6H_3$)^CH = 2,6-diphenyl-4-(2,5-dimethylphenyl)pyridine. This was synthesized from [Au{C^N(2,5-$Me_2C_6H_3$)^C}Cl] (283 mg, 0.50 mmol) and 4-methoxyphenylacetylene (99 mg, 0.75 mmol). Complex **2** was obtained as yellow crystals. Yield: 228 mg (69%). ^{1}H NMR (300 MHz, $CDCl_3$, 298 K)/ppm: δ 2.34 (s, 3H, −CH_3), 2.41 (s, 3H, −CH_3), 3.84 (s, 3H, −OCH_3), 6.88 (d, 2H, *J* = 7.0 Hz, −C≡CC_6H_4−), 7.13 (m, 2H, phenyl of C^N^C), 7.26 (m, 3H, −C_6H_3− and −C≡CC_6H_4−), 7.42 (m, 4H, −C_6H_3− and pyridine of C^N^C), 7.58 (m, 2H, phenyl of C^N^C), 8.15 (d, 2H, *J* = 7.0 Hz, phenyl of C^N^C). Positive FAB-MS: *m*/*z* 662 [M]$^+$. IR (KBr): 2152 cm^{-1}. (ν(C≡C)). Anal. Calcd for $C_{34}H_{26}AuNO$ (Found): C, 61.73 (61.40); H, 3.96 (3.95); N, 2.12 (2.07).

*[Au{C^N(2,5-$Me_2C_6H_3$)^C}(C≡C—C_6H_4—N(C_6H_5)$_2$-p)] (**3**).* This was synthesized from [Au{C^N(2,5-$Me_2C_6H_3$)^C}Cl] (283 mg, 0.50 mmol) and 4-diphenylaminophenylacetylene (202 mg, 0.75 mmol). Complex **3** was obtained as yellow crystals. Yield: 208 mg (52%). ^{1}H NMR (300 MHz, CD_2Cl_2, 298 K)/ppm: δ 2.32 (s, 3H, −CH_3), 2.38 (s, 3H, −CH_3), 7.01 (m, 4H, −N(C_6H_5)$_2$), 7.11 (m, 6H, phenyl of C^N^C and −C≡CC_6H_4−), 7.27 (m, 7H, −N(C_6H_5)$_2$ and −C_6H_3−), 7.42 (m, 3H, −C_6H_3− and phenyl of C^N^C), 7.47 (m, 3H, −C_6H_3− and pyridine of C^N^C), 7.62 (d, 2H, *J* = 7.6 Hz, phenyl of C^N^C), 8.05 (d, 2H, *J* = 7.6 Hz, phenyl of C^N^C). Positive FAB-MS: *m*/*z* 799 [M]$^+$. IR (KBr): 2143 cm^{-1} (ν(C≡C)). Anal. Calcd for $C_{46}H_{36}N_2Au\cdot 1/2H_2O$ (Found): C, 67.15 (66.79); H, 4.53 (4.16); N, 3.40 (3.49).

*[Au{C^N(4-^{t}BuC_6H_4)^C}(C≡C—C_6H_4—N(C_6H_5)$_2$-p)] (**4**).* HC^N-(4-^{t}BuC_6H_4)^CH = 2,6-diphenyl-4-(4-*tert*-butylphenyl)pyridine. This was synthesized from [Au{C^N(4-^{t}BuC_6H_4)^C}Cl] (297 mg, 0.50 mmol) and 4-diphenylaminophenylacetylene (202 mg, 0.75 mmol). Complex **4** was obtained as yellow crystals. Yield: 198 mg (48%). ^{1}H NMR (300 MHz, CD_2Cl_2, 298 K)/ppm: δ 1.38 (s, 9H, −^{t}Bu), 7.02 (m, 4H, −C≡CC_6H_4−), 7.09 (d, 4H, *J* = 8.5 Hz, phenyl of C^N^C), 7.27 (m, 6H, −N(C_6H_5)$_2$), 7.40 (m, 4H, −N(C_6H_5)$_2$), 7.60 (d, 2H, *J* = 8.5 Hz, phenyl of C^N^C), 7.71 (m, 6H, 4-^{t}BuC_6H_4 and pyridine of C^N^C), 8.03 (d, 2H, *J* = 8.5 Hz, phenyl of C^N^C). Positive FAB-MS: *m*/*z* 827 [M]$^+$. IR (KBr): 2127 cm^{-1} (ν(C≡C)). Anal. Calcd for $C_{47}H_{37}N_2Au$ (Found): C, 68.28 (68.14); H, 4.51 (4.57); N, 3.39 (3.37).

*[Au{C^N(4-^{i}PrC_6H_4)^C}(C≡C—C_6H_4—N(C_6H_5)$_2$-p)] (**5**).* HC^N-(4-^{i}PrC_6H_4)^CH = 2,6-diphenyl-4-(4-*iso*-propylphenyl)pyridine. This was synthesized from [Au{C^N(4-^{i}PrC_6H_4)^C}Cl] (290 mg, 0.50 mmol) and 4-diphenylaminophenylacetylene (202 mg, 0.75 mmol). Complex **5** was obtained as yellow crystals. Yield: 98 mg (24%). ^{1}H NMR (300 MHz, CD_2Cl_2, 298 K)/ppm: δ 1.13 (sep, 1H, −^{i}Pr), 1.30 (d, 6H, *J* = 7.1 Hz, −^{i}Pr), 7.02 (m, 4H, −C≡CC_6H_4−), 7.10 (d, 4H, *J* = 8.2 Hz, phenyl of C^N^C), 7.27 (m, 6H, −N(C_6H_5)$_2$), 7.37 (m, 2H, phenyl of C^N^C), 7.43 (m, 4H, −N(C_6H_5)$_2$), 7.71 (m, 6H, −C_6H_4− and pyridine of C^N^C), 8.02 (d, 2H, *J* = 8.2 Hz, phenyl of C^N^C). Positive FAB-MS: *m*/*z* 813 [M]$^+$. IR (KBr): 2135 cm^{-1} (ν(C≡C)). Anal. Calcd for $C_{46}H_{35}N_2Au\cdot 1/2H_2O$ (Found): C, 67.23 (67.11); H, 4.42 (4.32); N, 3.41 (3.42).

*[Au{C^N(4-FC_6H_4)^C}(C≡C—C_6H_4—OCH_3-p)] (**6**).* HC^N(4-FC_6H_4)^CH = 2,6-diphenyl-4-(4-fluorophenyl)pyridine. This was synthesized from [Au{C^N(4-FC_6H_4)^C}Cl] (278 mg, 0.50 mmol) and 4-methoxyphenylacetylene (99 mg, 0.75 mmol). Complex **6** was obtained as yellow crystals. Yield: 98 mg (30%). ^{1}H NMR (300 MHz, $CDCl_3$, 298 K)/ppm: δ 3.84 (s, 3H, −OCH_3), 6.89 (m, 2H, −C≡CC_6H_4−), 7.28 (m, 4H, −C≡CC_6H_4− and phenyl of C^N^C), 7.42 (t, 2H, *J* = 7.6 Hz, phenyl of C^N^C), 7.57 (d, 2H, *J* = 8.8 Hz, −C_6H_4F-4), 7.59 (s, 2H, pyridine of C^N^C), 7.64 (d, 2H, *J* = 7.6 Hz, phenyl of C^N^C), 7.74 (m, 2H, −C_6H_4F-4), 8.13 (d, 2H, *J* = 7.6 Hz, phenyl of C^N^C). Positive FAB-MS: *m*/*z* 651 [M]$^+$. IR (KBr): 2152 cm^{-1} (ν(C≡C)). Anal. Calcd for $C_{32}H_{21}AuFNO\cdot 2.5CH_2Cl_2$ (Found): C, 47.97 (48.00); H, 3.03 (2.62); N, 1.62 (1.82).

*[Au{C^N(C_6H_5)^C_{Np}}(C≡C—C_6H_4—N(C_6H_5)$_2$-p)] (**7**).* HC^N-(C_6H_5)^C_{Np}H = 2-(2-naphthyl)-4,6-diphenylpyridine. This was synthesized from [Au(C_6H_4—C^N^C_{Np})Cl] (294 mg, 0.50 mmol) and 4-diphenylaminophenylacetylene (202 mg, 0.75 mmol). Complex **7** was obtained as yellow crystals. Yield: 107 mg (26%). ^{1}H NMR (300 MHz, CD_2Cl_2, 298 K)/ppm: δ 7.04 (d, 4H, *J* = 7.4 Hz, −C≡CC_6H_4−), 7.07 (m, 1H, naphthyl of C^N^C), 7.13 (d, 4H, *J* = 7.4 Hz, −N(C_6H_5)$_2$), 7.29 (m, 4H, −N(C_6H_5)$_2$), 7.41 (m, 2H, −N(C_6H_5)$_2$), 7.46 (m, 2H, phenyl of C^N^C), 7.58 (m, 4H, naphthyl and phenyl of C^N^C), 7.72 (m, 2H, pyridine of C^N^C), 7.81 (m, 4H, −C_6H_5), 7.94 (m, 1H, −C_6H_5), 8.09 (d, 1H, *J* = 7.4 Hz, naphthyl of C^N^C), 8.22 (m, 1H, naphthyl of C^N^C), 8.43 (m, 1H, naphthyl of C^N^C). Positive FAB-MS: *m*/*z* 821 [M]$^+$. IR (KBr): 2139 cm^{-1} (ν(C≡C)). Anal. Calcd for $C_{47}H_{31}AuN_2\cdot 1/2CH_3CN$ (Found): C, 68.53 (68.38); H, 3.89 (3.63); N, 4.16 (4.13).

*[Au{C^N(2,5-$F_2C_6H_3$)^C_{Np}}(C≡C—C_6H_4—N(C_6H_5)$_2$-p)] (**8**).* HC^N-(2,5-$F_2C_6H_3$)^C_{Np}H = 4-(2,5-difluorophenyl)-2-(2-naphthyl)-6-phenylpyridine. This was synthesized from [Au{C^N(2,5-$F_2C_6H_3$)^C_{Np}}Cl] (312 mg, 0.50 mmol) and 4-diphenylaminophenylacetylene (202 mg, 0.75 mmol). Complex **8** was obtained as yellow crystals. Yield: 107 mg (25%). ^{1}H NMR (300 MHz, CD_2Cl_2, 298 K)/ppm: δ 7.01−7.08 (m, 5H, −C≡CC_6H_4− and naphthyl), 7.13 (m, 4H, −N(C_6H_5)$_2$), 7.20−7.32 (m, 8H, −N(C_6H_5)$_2$ and phenyl of C^N^C), 7.38 (m, 2H, phenyl of C^N^C), 7.47 (m, 2H, pyridine of C^N^C), 7.60 (d, 1H, *J* = 7.6 Hz, naphthyl of C^N^C), 7.63 (s, 1H, naphthyl of C^N^C), 7.75 (m, 2H, naphthyl of C^N^C), 7.83 (m, 1H, naphthyl of C^N^C), 8.02 (d, 1H, *J* = 7.6 Hz, −$C_6H_3F_2$-2,5), 8.08 (m, 1H, −$C_6H_3F_2$-2,5), 8.34 (m, 1H, −$C_6H_3F_2$-2,5). Positive FAB-MS: *m*/*z* 857 [M]$^+$. IR (KBr): 2143 cm^{-1} (ν(C≡C)). Anal. Calcd for $C_{47}H_{29}AuF_2N_2\cdot H_2O$ (Found): C, 64.53 (64.82); H, 3.57 (3.35); N, 3.20 (3.23).

*[Au{C^N(4-MeC_6H_4)^C_{Np}}(C≡C—C_6H_4—OCH_3-p)] (**9**).* HC^N(4-MeC_6H_4)^C_{Np}H = 4-(4-methylphenyl)-2-(2-naphthyl)-6-phenylpyridine. This was synthesized from [Au{C^N(4-MeC_6H_4)^C_{Np}}Cl] (301 mg, 0.50 mmol) and 4-methoxyphenylacetylene (99 mg, 0.75 mmol). Complex **9** was obtained as yellow crystals. Yield: 140 mg (40%). ^{1}H NMR (300 MHz, $CDCl_3$, 298 K)/ppm: δ 2.48 (s, 3H, −CH_3), 3.87 (s, 3H, −OCH_3), 6.92 (d, 2H, *J* = 8.5 Hz, −C≡CC_6H_4−), 7.38 (m, 4H, −C≡CC_6H_4− and −C_6H_4−), 7.45 (m, 2H, −C_6H_4−), 7.62 (m, 5H, phenyl and naphthyl of C^N^C), 7.70 (d, 2H, *J* = 8.1 Hz, pyridine of C^N^C), 7.75 (m, 1H, phenyl of C^N^C), 7.80 (m, 1H, phenyl of C^N^C), 8.08 (m, 1H, naphthyl of C^N^C), 8.13 (d, 1H, *J* = 7.1 Hz, naphthyl of C^N^C), 8.44 (m, 1H, naphthyl of C^N^C). Positive FAB-MS: *m*/*z* 698 [M]$^+$. IR (KBr): 2152 cm^{-1} (ν(C≡C)).

dx.doi.org/10.1021/ic4019212 | *Inorg. Chem.* 2013, 52, 12713−12725

Anal. Calcd for $C_{37}H_{26}AuNO\cdot 1/2H_2O$ (Found): C, 62.89 (62.86); H, 3.85 (4.12); N, 1.98 (2.05).

[Au(C_{Np}^N^C_{Np})(C≡C—C_6H_4—OCH_3-p)] (**10**). HC_{Np}^N^$C_{Np}H$ = 2,6-di-2-naphthylpyridine. This was synthesized from [Au(C_{Np}^N^C_{Np})Cl] (281 mg, 0.50 mmol) and 4-methoxyphenylacetylene (144 mg, 0.75 mmol). Complex **10** was obtained as yellow crystals. Yield: 144 mg (40%). ^{1}H NMR (300 MHz, $CDCl_3$, 298 K)/ppm: δ 3.90 (s, 3H, $-OCH_3$), 6.97 (d, 2H, J = 7.3 Hz, $-C{\equiv}CC_6H_4-$), 7.37 (m, 2H, $-C{\equiv}CC_6H_4-$), 7.48 (t, 2H, J = 8.0 Hz, naphthyl of C^N^C), 7.69 (m, 6H, naphthyl and pyridine of C^N^C), 7.82 (d, 2H, J = 8.0 Hz, naphthyl of C^N^C), 7.95 (m, 3H, naphthyl and pyridine of C^N^C), 8.46 (m, 2H, naphthyl of C^N^C). Positive FAB-MS: m/z 658 $[M]^+$. IR (KBr): 2137 cm^{-1} (ν(C≡C)). Anal. Calcd for $C_{34}H_{22}AuNO\cdot 1/2CH_3OH$ (Found): C, 61.52 (61.78); H, 3.56 (3.55); N, 2.08 (1.76).

[Au(C_{Np}^N^C_{Np})(C≡C—C_6H_4—N(C_6H_5)$_2$-p)] (**11**). This was synthesized from [Au(C_{Np}^N^C_{Np})Cl] (281 mg, 0.50 mmol) and 4-diphenylaminophenylacetylene (202 mg, 0.75 mmol). Complex **11** was obtained as yellow crystals. Yield: 91 mg (23%). ^{1}H NMR (300 MHz, $CDCl_3$, 298 K)/ppm: δ 7.07 (m, 2H, $-C{\equiv}CC_6H_4-$), 7.13 (m, 2H, $-C{\equiv}CC_6H_4-$), 7.19 (m, 4H, $-N(C_6H_5)_2$), 7.31–7.37 (m, 4H, $-N(C_6H_5)_2$), 7.46 (m, 2H, $-N(C_6H_5)_2$), 7.53 (m, 2H, naphthyl of C^N^C), 7.64 (m, 4H, naphthyl of C^N^C), 7.80 (d, 1H, J = 8.1 Hz, pyridine of C^N^C), 7.90 (m, 1H, pyridine of C^N^C), 7.95 (m, 2H, naphthyl of C^N^C), 8.44 (s, 2H, naphthyl of C^N^C). Positive FAB-MS: m/z 795 $[M]^+$. IR (KBr): 2143 cm^{-1} (ν(C≡C)). Anal. Calcd for $C_{45}H_{29}AuN_2\cdot 1/2H_2O$ (Found): C, 67.25 (67.37); H, 3.76 (3.60); N, 3.49 (3.48).

[Au{C_{Np}^N(2,5-$F_2C_6H_3$)^C_{Np}}(C≡C—C_6H_4—OCH_3-p)] (**12**). HC_{Np}^N(2,5-$F_2C_6H_3$)^$C_{Np}H$ = 4-(2,5-difluorophenyl)-2,6-di-2-naphthylpyridine. This was synthesized from [Au{C_{Np}^N(2,5-$F_2C_6H_3$)^C_{Np}}Cl] (337 mg, 0.50 mmol) and 4-methoxyphenylacetylene (99 mg, 0.75 mmol). Complex **12** was obtained as yellow crystals. Yield: 123 mg (32%). ^{1}H NMR (300 MHz, $CDCl_3$, 298 K)/ppm: δ 3.89 (s, 3H, $-OCH_3$), 6.93 (m, 2H, $-C{\equiv}CC_6H_4-$), 7.19 (m, 2H, naphthyl of C^N^C), 7.34 (m, 2H, $-C_6H_3F_2$-2,5), 7.46 (m, 3H, $-C_6H_3F_2$-2,5 and $-C{\equiv}CC_6H_4-$), 7.64 (m, 4H, naphthyl of C^N^C), 7.78 (m, 4H, naphthyl of C^N^C), 7.98 (s, 2H, pyridine of C^N^C), 8.42 (m, 2H, naphthyl of C^N^C). Positive FAB-MS: m/z 770 $[M]^+$. IR (KBr): 2151 cm^{-1} (ν(C≡C)). Anal. Calcd for $C_{40}H_{24}AuF_2NO\cdot 3H_2O$ (Found): C, 58.33 (58.21); H, 3.67 (3.30); N, 1.70 (1.66).

[Au{C_{Np}^N(2,5-$F_2C_6H_3$)^C_{Np}}(C≡C—C_6H_4—N(C_6H_5)$_2$-p)] (**13**). This was synthesized from [Au{C_{Np}^N(2,5-$F_2C_6H_3$)^C_{Np}}Cl] (337 mg, 0.50 mmol) and 4-diphenylaminophenylacetylene (202 mg, 0.75 mmol). Complex **13** was obtained as yellow crystals. Yield: 63 mg (14%). ^{1}H NMR (300 MHz, $CDCl_3$, 298 K)/ppm: δ 7.09 (d, 4H, J = 8.4 Hz, $-C{\equiv}CC_6H_4-$), 7.18 (m, 6H, $-N(C_6H_5)_2$ and naphthyl of C^N^C), 7.27 (m, 6H, $-N(C_6H_5)_2$ and naphthyl of C^N^C), 7.34 (m, 5H, $-C_6H_3F_2$-2,5 and naphthyl of C^N^C), 7.44 (m, 2H, naphthyl of C^N^C),7.54 (m, 2H, naphthyl of C^N^C), 7.66 (m, 2H, naphthyl of C^N^C), 7.78 (s, 2H, pyridine of C^N^C), 7.98 (m, 1H, $-C_6H_3F_2$-2,5), 8.42 (s, 1H, $-C_6H_3F_2$-2,5). Positive FAB-MS: m/z 907 $[M]^+$. IR (KBr): 2137 cm^{-1} (ν(C≡C)). Anal. Calcd for $C_{51}H_{31}AuF_2N_2$ (Found): C, 67.55 (67.15); H, 3.45 (3.47); N, 3.09 (3.25).

[Au(dhpbzq)(C≡C—C_6H_4—OCH_3-p)] (**14**). dhpbzq = 5,6-dihydro-2-phenylbenzo[*h*]quinoline. This was synthesized from [Au(dhpbzq)Cl] (244 mg, 0.50 mmol) and 4-methoxyphenylacetylene (99 mg, 0.75 mmol). Complex **14** was obtained as yellow crystals. Yield: 172 mg (59%). ^{1}H NMR (400 MHz, $CDCl_3$, 298 K)/ppm: δ 3.01 (m, 4H, $-CH_2-$ of dhpbzq), 3.83 (s, 3H, $-OCH_3$), 6.86 (m, 2H, $-C{\equiv}CC_6H_4-$), 7.00 (m, 1H, phenyl of dhpbzq), 7.31 (m, 2H, $C{\equiv}CC_6H_4$), 7.35(m, 1H, phenyl of dhpbzq), 7.39 (m, 1H, phenyl of dhpbzq), 7.52 (m, 1H, phenyl of dhpbzq), 7.54–7.58 (m, 3H, phenyl of dhpbzq), 7.60 (m, 1H, phenyl of dhpbzq), 7.84 (d, 1H, J = 7.2 Hz, pyridine of dhpbzq), 8.10 (d, J = 7.2 Hz, pyridine of dhpbzq). Positive FAB-MS: m/z 583 $[M]^+$. IR (KBr): 2143 cm^{-1} (ν(C≡C)). Anal. Calcd for $C_{28}H_{20}AuNO$ (Found): C, 57.64 (57.40); H, 3.46 (3.46); N, 2.40 (2.46).

[Au(dhpbzq)(C≡C—C_6H_4—N(C_6H_5)$_2$-p)] (**15**). This was synthesized from [Au(dhpbzq)Cl] (244 mg, 0.50 mmol) and 4-diphenylaminophenylacetylene (202 mg, 0.75 mmol). Complex **15** was obtained as yellow crystals. Yield: 112 mg (31%). ^{1}H NMR (400 MHz, $CDCl_3$, 298 K)/ppm: δ 1.27 (t, 3H, J = 3.0 Hz, ethyl), 2.65 (q, 2H, ethyl), 3.04 (m, 4H, CH_2 of dhpbzq), 6.99 (d, 1H, J = 7.5 Hz, phenyl of dhpbzq), 7.16 (d, 2H, J = 6.1 Hz, $-C{\equiv}CC_6H_4-$), 7.23 (m, 1H, phenyl of dhpbzq), 7.28 (m, 1H, phenyl of dhpbzq), 7.33 (m, 3H, $-C{\equiv}CC_6H_4-$ and phenyl of dhpbzq), 7.53 (m, 2H, pyridine of dhpbzq), 7.59 (m, 1H, pyridine of dhpbzq), 7.82 (d, 1H, J = 7.5 Hz, phenyl of dhpbzq), 8.08 (d, 1H, J = 7.5 Hz, phenyl of dhpbzq). Positive FAB-MS: m/z 721 $[M]^+$. IR (KBr): 2137 cm^{-1} (ν(C≡C)). Anal. Calcd for $C_{39}H_{27}AuN_2$ (Found): C, 65.00 (64.91); H, 3.78 (3.78); N, 3.89 (3.89).

[Au(dhpbzq)(C≡C—C_6H_4—C_2H_5-p)] (**16**). This was synthesized from [Au(dhpbzq)Cl] (244 mg, 0.50 mmol) and 4-ethylphenylacetylene (98 mg, 0.75 mmol). Complex **16** was obtained as pale yellow crystals. Yield: 102 mg (35%). ^{1}H NMR (400 MHz, $CDCl_3$, 298 K)/ppm: δ 1.30 (m, 3H, $-CH_3$), 2.64 (m, 2H, $-CH_2-$), 3.04 (m, 4H, $-CH_2-$ of dhpbzq), 6.98 (d, 1H, J = 7.5 Hz, phenyl of dhpbzq), 7.16 (d, 2H, J = 6.1 Hz, $C{\equiv}CC_6H_4$), 7.24 (m, 1H, phenyl of dhpbzq), 7.28–7.37 (m, 4H, $C{\equiv}CC_6H_4$ and phenyl of dhpbzq), 7.53 (m, 2H, phenyl of dhpbzq), 7.58 (d, 1H, J = 7.5 Hz, phenyl of dhpbzq), 7.82 (d, 1H, J = 7.5 Hz, pyridine of dhpbzq), 8.08 (d, 1H, J = 7.5 Hz, pyridine of dhpbzq). Positive FAB-MS: m/z 582 $[M]^+$. IR (KBr): 2129 cm^{-1} (ν(C≡C)). Anal. Calcd for $C_{29}H_{22}AuN$ (Found): C, 59.90 (59.88); H, 3.81 (4.00); N, 2.41 (2.42).

[Au(C_6H_5-dhpbzq)(C≡C—C_6H_4—OCH_3-p)] (**17**). C_6H_5-dhpbzq = 5,6-dihydro-2,4-diphenylbenzo[*h*]quinoline. This was synthesized from [Au(C_6H_5-dhpbzq)Cl] (282 mg, 0.50 mmol) and 4-methoxyphenylacetylene (99 mg, 0.75 mmol). Complex **17** was obtained as yellow crystals. Yield: 168 mg (51%). ^{1}H NMR (300 MHz, $CDCl_3$, 298 K)/ppm: δ 2.97 (m, 4H, $-CH_2-$ of C_6H_5-dhpbzq), 3.84 (s, 3H, $-OCH_3$), 6.88 (d, 2H, J = 8.8 Hz, $-C{\equiv}CC_6H_4-$), 6.97 (d, 1H, J = 7.0 Hz, phenyl of C_6H_5-dhpbzq), 7.20 (m, 1H, phenyl of C_6H_5-dhpbzq), 7.32 (m, 2H, $-C{\equiv}CC_6H_4-$), 7.37 (m, 2H, phenyl of C_6H_5-dhpbzq), 7.44 (dd, 2H, J = 2.1 and 7.2 Hz, $-C_6H_4-$ of C_6H_5-dhpbzq), 7.54 (m, 4H, C_6H_4 and phenyl of C_6H_5-dhpbzq), 7.61 (s, 1H, pyridine of C_6H_5-dhpbzq), 7.84 (d, 1H, J = 7.2 Hz, phenyl of C_6H_5-dhpbzq), 8.10 (d, 1H, J = 7.2 Hz, phenyl of C_6H_5-dhpbzq). Positive FAB-MS: m/z 660 $[M]^+$. IR (KBr): 2147 cm^{-1} (ν(C≡C)). Anal. Calcd for $C_{34}H_{24}AuNO$ (Found): C, 61.92 (61.89); H, 3.67 (3.73); N, 2.12 (2.15).

[Au(2,5-$F_2C_6H_3$-dhpbzq)(C≡C—C_6H_4—OCH_3-p)] (**18**). 2,5-$F_2C_6H_3$-dhpbzq = 4-(2,5-difluorophenyl)-5,6-dihydro-2-phenylbenzo[*h*]quinoline. This was synthesized from [Au(2,5-$F_2C_6H_3$-dhpbzq)Cl] (300 mg, 0.50 mmol) and 4-methoxyphenylacetylene (99 mg, 0.75 mmol). Complex **18** was obtained as yellow crystals. Yield: 160 mg (46%). ^{1}H NMR (300 MHz, $CDCl_3$, 298 K)/ppm: δ 2.84 (m, 2H, $-CH_2-$ of dhpbzq), 2.99 (m, 2H, $-CH_2-$ of 2,5-$F_2C_6H_3$-dhpbzq), 3.84 (s, 3H, $-OCH_3$), 6.87 (d, 2H, J = 8.8 Hz, $-C{\equiv}CC_6H_4-$), 6.99 (d, 1H, J = 6.6 Hz, phenyl of 2,5-$F_2C_6H_3$-dhpbzq), 7.10 (m, 1H, $-C_6H_3F_2$-2,5), 7.19 (m, 2H, $-C{\equiv}CC_6H_4-$), 7.36 (m, 4H, phenyl of 2,5-$F_2C_6H_3$-dhpbzq), 7.51 (s, 1H, pyridine of 2,5-$F_2C_6H_3$-dhpbzq), 7.58 (m, 2H, phenyl of 2,5-$F_2C_6H_3$-dhpbzq), 7.85 (d, 1H, J = 6.6 Hz, 2,5-$F_2C_6H_3$-dhpbzq), 8.10 (d, 1H, J = 6.6 Hz, $-C_6H_3F_2$-2,5). Positive FAB-MS: m/z 696 $[M]^+$. IR (KBr): 2152 cm^{-1} (ν(C≡C)). Anal. Calcd for $C_{34}H_{22}AuF_2NO$ (Found): C, 58.71 (58.35); H, 3.19 (3.33); N, 2.01 (1.95).

■ ASSOCIATED CONTENT

Ⓢ Supporting Information

EL spectra and device performance of **4**. Crystal structures of **1** and **6**, in CIF format. This material is available free of charge via the Internet at http://pubs.acs.org.

■ AUTHOR INFORMATION

Corresponding Author

*E-mail: chanmym@hku.hk (M.-Y.C.), wwyam@hku.hk (V.W.-W.Y.).

Notes

The authors declare no competing financial interest.

■ ACKNOWLEDGMENTS

V. W.-W. Y. acknowledges support from The University of Hong Kong and the URC Strategic Research Theme on New Materials. This work has been supported by the University Grants Committee Areas of Excellence Scheme (AoE/P-03/08) and the General Research Fund (GRF) (HKU 7063/10P), both from the Research Grants Council of Hong Kong Special Administrative Region, P. R. China. V. K.-M. A. acknowledges the receipt of a postdoctoral fellowship and the support from the URC Small Project Funding, both administered by the University of Hong Kong. D. P.-K. T. acknowledges the receipt of a postgraduate studentship from The University of Hong Kong. We also thank Dr. L. Szeto for technical assistance in crystal structure determination, as well as Prof. Z.-Y. Zhou, Dr. W. T.-K. Chan, and the Hong Kong Polytechnic University for X-ray data collection of complex **6**.

■ REFERENCES

(1) (a) Schmidbaur, H. *Chem. Soc. Rev.* **1995**, *24*, 391. (b) Hutchings, G. J.; Brust, M.; Schmidbaur, H. *Chem. Soc. Rev.* **2008**, *37*, 1759.
(2) (a) Ford, P. C.; Vogler, A. *Acc. Chem. Res.* **1993**, *26*, 220. (b) Vogler, A.; Kunkely, H. *Coord. Chem. Rev.* **2001**, *219*−*221*, 489.
(3) Fung, E. Y.; Olmstead, M. M.; Vickery, J. C.; Balch, A. L. *Coord. Chem. Rev.* **1998**, *171*, 151.
(4) Burini, A.; Mohamed, A. A.; Fackler, J. P., Jr. *Comments Inorg. Chem.* **2003**, *24*, 253.
(5) Puddephatt, R. J. *Chem. Soc. Rev.* **2008**, *37*, 2012.
(6) Pyykkö, P. *Chem. Rev.* **1988**, *88*, 563.
(7) (a) Yam, V. W.-W.; Cheng, E. C.-C. *Top. Curr. Chem.* **2007**, *281*, 269. (b) Yam, V. W.-W.; Cheng, E. C.-C. *Chem. Soc. Rev.* **2008**, *37*, 1806.
(8) (a) Baldo, M. A.; O'Brien, D. F.; You, Y.; Shoustikovm, A.; Sibley, S.; Thompson, M. E.; Forrest, S. R. *Nature* **1998**, *395*, 151. (b) Baldo, M. A.; Lamansky, S.; Thompson, M. E.; Forrest, S. R. *Appl. Phys. Lett.* **1999**, *75*, 4. (c) Baldo, M. A.; Thompson, M. A.; Forrest, S. R. *Nature* **2000**, *403*, 750.
(9) Adachi, C.; Kwong, R. C.; Djurovich, P.; Adamovich, V.; Baldo, M. A.; Thompson, M. E.; Forrest, S. R. *Appl. Phys. Lett.* **2001**, *79*, 2082. (b) Lamansky, S.; Djurovich, P. I.; Abdel-Razzaq, F.; Garon, S.; Murphy, D. L.; Thompson, M. E. *J. Appl. Phys.* **2002**, *92*, 1570.
(10) (a) Cocchi, M.; Virgili, D.; Fattori, V.; Rochester, D. L.; Williams, J. A. G. *Adv. Funct. Mater.* **2007**, *17*, 285. (b) Cocchi, M.; Kalinowski, J.; Murphy, L.; Williams, J. A. G.; Fattori, V. *Org. Electron.* **2010**, *11*, 388. (c) Cocchi, M.; Kalinowski, J.; Fattori, V.; Williams, J. A. G.; Murphy, L. *Appl. Phys. Lett.* **2009**, *94*, 073309.
(11) Kui, S. C.-F.; Sham, I. H.-T.; Cheung, C. C.-C.; Ma, C.-W.; Yan, B.; Zhu, N.; Che, C.-M.; Fu, W.-F. *Chem.—Eur. J.* **2006**, *13*, 417.
(12) Tam, A. Y.-Y.; Tsang, D. P.-K.; Chan, M.-Y.; Zhu, N.; Yam, V. W.-W. *Chem. Commun.* **2011**, *47*, 3383.
(13) (a) Tung, Y.-L.; Wu, P.-C.; Liu, C.-S.; Chi, Y.; Yu, J.-K.; Hu, Y.-H.; Chou, P.-T.; Peng, S.-M.; Lee, G.-H.; Tao, Y.; Carty, A. J.; Shu, C.-F.; Wu, F.-I. *Organometallics* **2004**, *23*, 3745. (b) Lee, T.-C.; Hung, J.-Y.; Chi, Y.; Cheng, Y.-M.; Lee, G.-H.; Chou, P.-T.; Chen, C.-C.; Chang, C.-H.; Wu, C.-C. *Adv. Funct. Mater.* **2009**, *19*, 2639.
(14) Bernhard, S.; Barron, J. A.; Houston, P. L.; Abruña, H. D.; Ruglovksy, J. L.; Gao, X.; Malliaras, G. G. *J. Am. Chem. Soc.* **2002**, *124*, 13624.
(15) Yam, V. W.-W.; Choi, S. W.-K.; Lai, T.-F.; Lee, W.-K. *J. Chem. Soc., Dalton Trans.* **1993**, 1001.
(16) (a) Yam, V. W.-W.; Wong, K. M.-C.; Hung, L.-L.; Zhu, N. *Angew. Chem., Int. Ed.* **2005**, *117*, 3167. (b) Wong, K. M.-C.; Zhu, X.; Hung, L.-L.; Zhu, N.; Yam, V. W.-W.; Kwok, H.-S. *Chem. Commun.* **2005**, 2906. (c) Wong, K. M.-C.; Hung, L.-L.; Lam, W. H.; Zhu, N.; Yam, V. W.-W. *J. Am. Chem. Soc.* **2007**, *129*, 4350. (d) Au, V. K.-M.; Wong, K. M.-C.; Zhu, N.; Yam, V. W.-W. *J. Am. Chem. Soc.* **2009**, *131*, 9076. (e) Au, V. K.-M.; Wong, K. M.-C.; Tsang, D. P.-K.; Chan, M.-Y.; Zhu, N.; Yam, V. W.-W. *J. Am. Chem. Soc.* **2010**, *132*, 14273. (f) Tang, M.-C.; Tsang, D. P.-K.; Chan, M.-Y.; Wong, K. M.-C.; Yam, V. W.-W. *Angew. Chem., Int. Ed.* **2013**, *1*, 446. (g) Au, V. K.-M.; Zhu, N.; Yam, V. W.-W. *Inorg. Chem.* **2013**, *52*, 558.
(17) (a) Au, V. K.-M.; Wong, K. M.-C.; Zhu, N.; Yam, V. W.-W. *Chem.—Eur. J.* **2011**, *17*, 130. (b) Lu, W.; Chan, K. T.; Wu, S.-X.; Chen, Y.; Che, C.-M. *Chem. Sci.* **2012**, *3*, 752. (c) Au, V. K.-M.; Lam, W. H.; Wong, W.-T.; Yam, V. W.-W. *Inorg. Chem.* **2012**, *51*, 7537.
(18) Wong, K.-H.; Cheung, K.-K.; Chan, M. C.-W.; Che, C.-M. *Organometallics* **1998**, *17*, 3505.
(19) (a) Marcon, G.; Carotti, S.; Coronnello, M.; Messori, L.; Mini, E.; Orioli, P.; Mazzei, T.; Cinellu, M. A.; Minghetti, G. *J. Med. Chem.* **2002**, *45*, 1672. (b) Casini, A.; Cinellu, M. A.; Minghetti, G.; Gabbiani, C.; Coronnello, M.; Mini, E.; Messori, L. *J. Med. Chem.* **2006**, *49*, 5524.
(20) (a) Ichimura, K.; Kobayashi, T.; King, K. A.; Watts, R. J. *J. Phys. Chem.* **1987**, *91*, 6104. (b) Wang, X. Y.; Prabhu, R. N.; Schmehl, R. H.; Weck, M. *Macromolecules* **2006**, *39*, 3140.
(21) Chen, F.-Q.; Yu, Q.; Guo, Y.; Fan, M.-G. *Sci. China, Ser. B: Chem.* **1991**, *34*, 135.
(22) Shoute, L. C. T.; Neta, P. *J. Phys. Chem.* **1990**, *94*, 2447.
(23) Joschek, H.-I.; Grossweiner, L. I. *J. Am. Chem. Soc.* **1966**, *88*, 3261.
(24) Komamine, S.; Fujitsuka, M.; Ito, O. *Phys. Chem. Chem. Phys.* **1999**, *1*, 4745.
(25) Kröhnke, F. *Synthesis* **1976**, 1.
(26) McIlroy, S. P.; Cló, E.; Nikolajsen, L.; Frederiksen, P. K.; Nielsen, C. B.; Mikkelsen, K. V.; Gothelf, K. V.; Ogilby, P. R. *J. Org. Chem.* **2005**, *70*, 1134.
(27) (a) Demas, J. N.; Crosby, G. A. *J. Phys. Chem.* **1971**, *75*, 991. (b) van Houten, J.; Watts, R. *J. Am. Chem. Soc.* **1976**, *98*, 4853.
(28) Connelly, N. G.; Geiger, W. E. *Chem. Rev.* **1996**, *96*, 877.
(29) *SAINT+. SAX Area Detector Integration Program. Version 7.34A*; Bruker AXS, Inc.: Madison, WI, 2006.
(30) Sheldrick, G. M. *SADABS, Empirical Absorption Correction Program*; University of Göttingen: Göttingen, Germany, 2004.
(31) Sheldrick, G. M. *SHELXS 97: Programs for Crystal Structure Analysis (Release 97-2)*; University of Göttingen: Göttingen, Germany, 1997.